SJÄLVSTÄNDIGA ARBETEN I MATEMATIK

MATEMATISKA INSTITUTIONEN, STOCKHOLMS UNIVERSITET

Quantum Nonlocality in Star-Network Entanglement Swapping Configurations

av

Armin Tavakoli

2014 - No 14

MATEMATISKA INSTITUTIONEN, STOCKHOLMS UNIVERSITET, 106 91 STOCKHOLM

Quantum Nonlocality in Star-Network Entanglement Swapping Configurations

Armin Tavakoli

Självständigt arbete i matematik 15 högskolepoäng, Grundnivå

Handledare: Antonio Acín och Rikard Bøgvad

2014

Quantum Nonlocality in Star-Network Entanglement Swapping Configurations

Armin Tavakoli
ICFO - Institute of Photonic Science
Stockholm University
Bachelor Thesis

May 31, 2014

Supervisor:
Antonio Acín

Assistant supervisors:
Rikard Bögvad

Abstract

Entanglement swapping is a quantum mechanical process in which spatially separated initially independent entangled quantum systems can be subject to nonlocal correlations. This thesis aims to study quantum correlations in entanglement swapping scenarios in a broad class of star-networks. We introduce a nonlinear assumption of local realism from which we characterize classical correlations. We present new Bell inequalities for entanglement swapping configurations in several star-networks and show that our inequalities are tight with respect to local realist correlations. In addition we show how to close the freedom-of-choice loophole. Quantum violations are provided for our inequalities and their various properties are extensively studied. Furthermore we study the behaviour of quantum correlations in the presence of experimental imperfections restricted to inefficient detectors and white noise tolerance.

Acknowledgements

First I want to thank my supervisor Antonio Acín for introducing me to research in theoretical physics, making me a part of his group and a part of ICFO and providing me with financial support for my first two internships making my stay in Barcelona possible. Due to Antonio opening the door for me, I had the opportunity of conducting my third internship with Maciej Lewenstein in the quantum optics theory group to whom I owe gratitude for financial support. I also thank the people in the Acín-group involved with the project, firstly Paul Skrzypczyk for all his support and active guidance during the course of this project. Paul also deserves proper credit for programing the SDPs used for numerical analysis. I jointly thank Paul Skrzypczyk and Daniel Cavalcanti for discussions and for always taking the time to answer my questions, especially the irrelevant and stupid questions since these are undoubtly the most important ones.

Contents

1 Introduction

It is often said that the theory of quantum mechanics provides a counter-intuitive view of nature. Two fundamental properties of nature that have been shown cannot both be true in a reality described by quantum mechanics is 1) Locality – that two space-like separated events are independent of each other and 2) Realism – that physical entities have real predictable and well defined properties independent of observation. In contrast to quantum mechanics, locality and realism are profound principles of classical physics. This fundamental discrepancy between the quantum and the classical description calls for directing some attention at fundamental physics and quantum theory.

1.1 Historical background: EPR and quantum correlations

In the early days of quantum mechanics, its radical view of nature lead to a conflict with the established classical ideas of nature. In 1935 a famous paper was published by Einstein, Podolsky and Rosen (EPR) entitled "*Can Quantum-Mechanical description of physical reality be considered complete?*" where the authors argued that quantum mechanics could not be considered a complete theory [1]. EPR used quantum mechanical formalism to show the existence of two-particle states subject to perfect correlations in both position and momentum even though both particles were spatially separated and non-interacting. These EPR-states are today more commonly called entangled states, a term coined by Schrödinger to emphasize the inability to treat the systems independently [2]. According to quantum theory, an accurate measurement of position or momentum (but not both due to Heisenberg's uncertainty relation) on one particle provides accurate knowledge about the outcome of the analog measurement performed on the second particle. On this basis, EPR concluded that the second particle must have had well-defined physical properties a priori to measurement. Since quantum mechanics fails to provide this a priori knowledge EPR argued that quantum mechanics must be an incomplete theory and emphasized the need of completing it.

The conflict between quantum mechanics and the EPR-argument was essentially a problem of metaphysics until 1964 when John S. Bell published a groundbreaking paper "*On the Einstein Podolsky Rosen paradox*". Bell imposed completeness in the sense of EPR by providing each particle with a local hidden variable, imagined to be carried with the particles under separation. Given the hidden variable and a measurement, an outcome can be predicted with a probability of unity. Such Local Hidden[1] Variable theories (LHVs) are synonymous to models enforcing the assumptions of locality and realism (local realism). Bell showed that despite LHVs being able to reproduce some correlations predicted by quantum mechanics, there exists quantum correlations that are impossible for the entire family of LHVs to reproduce [3]. Bell's work provides an observable difference between the predictions of quantum theory and the EPR-argument. It is enforced through Bell's inequality, quantifying the correlations attainable with any LHV model. Quantum mechanics on the other hand, allows for violations of Bell's inequality and therefore claims that at least one of the assumptions of locality and realism made by EPR are false. In conclusion the discrepancy between quantum mechanics and the EPR-argument could be settled by experiments.

Experimental tests of the predictions of quantum theory are usually not based Bell's original inequality but on more general inequality due to Clauser-Horne-Shimony-Holt (CHSH) more suitable to experimental tests [4]. The prediction of nonlocal (quantum) correlations was confirmed by a first generation of experiments violating the CHSH-inequality [5, 6]. However, these early experimental tests where subject to various experimental loopholes, most notably 1) the detection loophole arising from imperfect detectors and 2) the locality loophole arising from not having space-like separated measurement events. There is also theoretical loopholes such as the freedom-of-choice loophole arising from the metaphysical problem of superdeterminism related to free will of choosing measurement settings. A second generation of tests of the CHSH-inequality have successfully closed each loophole individually [7, 8, 9, 10, 11, 12]. Nevertheless no one experiment has been able to close all loopholes simultaneously.

In conclusion, there is very strong experimental evidence supporting the validity of Bell's theorem, the rejection of at least one of the principles of locality and realism[2] and the existence of quantum nonlocal correlations in nature.

[1]The name "hidden" variable theory is due to historical reasons. There is nothing forcing the hidden variable to actually be hidden from the observer.

[2]More recent work shows that a broad class of nonlocal realist theories are incompatible with experimentally observed quantum correlations thus suggesting that abandoning the principle of locality may not be sufficient [13].

1.2 Motivation and outline of thesis

The existence of Bell inequalities and their numerous successful experimental violations are important and fundamental results in quantum mechanics. The advances in the studies of correlations between outcomes in measurement scenarios have led to remarkable progress in both applications based on the power of quantum entanglement in comparison to classical tools and theoretical understanding of the foundations of quantum mechanics. Pioneer experimentalist in the field Alain Aspect expresses the evolution of the field as:

> *"But in an unexpected way, it has been discovered that entanglement also offers completely new possibilities in the domain of information treatment and transmission. A new field has emerged, broadly called Quantum Information, which aims to implement radically new concepts that promise surprising applications".* [14]

In terms of practical applications the studies of quantum correlations has led to e.g. 1) quantum key distribution and quantum cryptography [15, 16] allowing for detection of eavesdroppers [17, 18], 2) reduction of communication complexity [19], 3) quantum computing [20] and 4) device independent entanglement witness [21, 22].

Usually studies of correlations of measurement outcomes begin at the Bell scenario with two parties performing measurements on a shared entangled state. However one can construct many other scenarios exploiting quantum nonlocality than the ordinary Bell scenario. In comparison, very little attention has been directed at such systems so far. Nevertheless the reasearch interest has increased significantly during the last years. There are many motivations to why more complicated networks are interesting. Let's present at least three of them: 1) The fast experimental progress on quantum communication networks and emerging quantum information technologies based on distribution of entangled states makes the study of quantum nonlocality in large networks of high complexity interesting [23]. These systems rely on distribution of several bipartite states and one or more parties performing joint measurements yielding quantum correlations through entanglement swapping. 2) The conceptual motivation is mainly focused on the nonlocality properties of correlations generated through the process of entanglement swapping which is profoundly related to quantum teleportation and is not well understood today [24]. Finding Bell-type inequalities for such entangle-

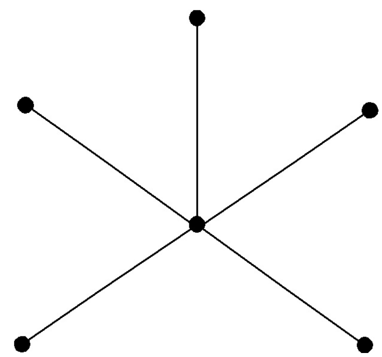

Figure 1: Star-network with five edges and six vertices.

ment swapping networks configurations and studying the quantum properties with respect to different important experimental parameters such as detection efficiency and tolerance of white-noise is of interest for both foundational and experimental purposes. 3) During the last couple of years research interest has been directed to study quantum foundations in terms of causal networks (bayesian networks). Bayesian networks has for several decades been an active research field in both mathematical statistics and computer science. However the properties of these networks has always been taken classical. Recent efforts has taken the first steps to analyzing bayesian networks subject to quantum nonlocality and thus establishing closer relationships between both the concepts and the fields [25, 26, 27, 28].

The work presented in this thesis considers a class of networks in a broad sense represented by star-graphs where each edge in the graph represents a shared entangled state and each vertex represents a party performing a measurement on one part of the shared state (see figure 1 for example). The simplest form of such star-networks, with three parties performing two-outcome measurements has been studied in [33, 30] showing interesting properties with respect to the Bell scenario. This thesis aims to generalize the known results for star-network entanglement swapping configurations by studying many-party star-networks with multipartite sources and high state-dimensions. Having provided some background in section 1, we will give a short introduction to fundamental quantum theory in section 2. In section 3 we properly introduce definitions and mathematically postulate local realism in star-networks. We will argue the relevance of this postulate since it is essential for our studies. Section 4 will contain several new Bell inequalities, the relevance of each motivated. Also, we prove characteristics of our inequalities with respect to local realist correlations. In addition we show how to theoretically close the freedom-of-choice loophole protecting our theory from assumptions of superdeterminism. Section 4 is for extensive numerical studies of the presented Bell inequalities. We will consider various case studies, most importantly demonstrating quantum violations of our inequalities. In section 5 we will use the intuition obtained from the numerical studies to give an analytical framework for analyzing quantum properties of our inequalities. This includes giving proofs of maximal violations. In section 6 we study the behavior of quantum correlations in real experimental scenarios where inefficient detection and noisy environments have to be taken into account. Section 7 provides a summary, conclusions and open questions.

2 Background in quantum mechanics

Quantum mechanics constitutes a mathematical framework for theories of physical reality. It fundamentally relies on a set of postulates connecting nature to the formalism of quantum theory. We will only be concerned with two of the postulates.

Postulate: (Quantum state). To every physical system that is isolated from the environment a state space of the system represented by a hilbert space is associated. The physical system is completely described by its state which is a unit vector in the state space of the system.

In introductory quantum mechanics the postulates are expressed in the quantum state vector representations. However they have a more general formulation in the language of density operators [20]. In many common scenarios encountered in quantum mechanics, e.g. when considering quantum systems that randomly output various states one needs to go beyond the state vector description and introduce the notion of a density operator.

2.1 Density operators

Let S be a source and let $\{p_i \big| |\psi_i\rangle\}_{i=1}^N$ be a set of probabilities and states such that S outputs the state $|\psi_i\rangle$with probability p_i. The set$\{p_i \big| |\psi_i\rangle\}_{i=1}^N$ is referred to as a *mixed ensemble* and is associated to a *density matrix* (or equivalently *density operator*) ρ.

$$\rho \equiv \sum_{i=1}^{N} p_i |\psi_i\rangle\langle\psi_i| \tag{1}$$

In the special case of $N = 1$ the density matrix is said to be *pure* since the same state vector is outputted with unity probability. We state two characterizing properties of any density matrix:

1. ρ has unit trace.

2. ρ is a hermitian positive semi-definit operator.

Although not provided here it is straightforward to prove these two properties from (1).

2.2 Measurements

At the heart of quantum mechanics is the concept of measurement. This is postulated as follows in terms of density matrices:

Postulate: (Quantum measurement). Quantum measurements are described by a set $\{M_m\}$ of measurement operators with the index m referring to the outcome of the measurement. The collection of measurement operators satisfy

$$\sum_m M_m^\dagger M_m = \mathbf{1} \tag{2}$$

where $\mathbf{1}$ is the identity operator. If the state of the quantum system is ρ immediately before measurement then the probability of obtaining the outcome m when performing the measurement M_m is

$$P(m|M_m) = \mathrm{Tr}(M_m^\dagger M_m \rho) \tag{3}$$

and the state of the system immediately after the measurement is

$$\rho_{postM_m} = \frac{M_m \rho M_m^\dagger}{\mathrm{Tr}(M_m^\dagger M_m \rho)} \tag{4}$$

In elementary quantum mechanics one usually considers projective measurements where the measurement operators are orthogonal projectors. However the postulate allows for more general measurements often referred to as *positive operator valued measurements* (POVMs) obeying (2).

One should also be familiar with the three *Pauli matrices* since these often occur in measurements involving qubits. The Pauli matrices together with the identity operator span the space of 2×2 hermitian matrices.

$$\mathbf{1} = \begin{pmatrix} 1 & 0 \\ 0 & 1 \end{pmatrix} \quad \sigma_x = \begin{pmatrix} 0 & 1 \\ 1 & 0 \end{pmatrix} \quad \sigma_y = \begin{pmatrix} 0 & -i \\ i & 0 \end{pmatrix} \quad \sigma_z = \begin{pmatrix} 1 & 0 \\ 0 & -1 \end{pmatrix} \tag{5}$$

Observe that all Pauli matrices are traceless, hermitian and unitary and that the square of any Pauli matrix is identity.

2.3 Separable and entangled states

Consider a composite system with a hilbert space $\mathscr{H}$ equipped with subsystems with hilbert spaces $\mathscr{H}_A$ and $\mathscr{H}_B$ respectively. Let the composite state of the system be described by a density matrix ρ^{AB}. The reduced state describing one part of the composite system, ρ^A, can be obtained from 'tracing out' the second subsystem by employing a *partial trace*

$$\rho^A = \mathrm{Tr}_B\left(\rho^{AB}\right) = \sum_i \langle i|\rho^{AB}|i\rangle \tag{6}$$

where the set $\{|i\rangle\}$ constitutes an ON-basis of $\mathscr{H}_B$. The reduced state of the second part of the composite system, ρ^B, can be defined in an analogy with (6).

Since the density matrix ρ^{AB} is a non-negative operator a spectral decomposition can be performed

$$\rho^{AB} = \sum_i \lambda_i |i\rangle\langle i| \tag{7}$$

where λ_i are non-negative real numbers associated to the eigenvector $|i\rangle$. Due to the unit trace property of density matrices the sum of the coefficients λ_i equals unity. The composite system associated to ρ^{AB} is a *separable* state if and only if it is an element in the convex hull of product states

$$\rho^{AB} = \sum_i p_i \rho_i^A \otimes \rho_i^B \tag{8}$$

where $p_i > 0$ and ρ_i^A and ρ_i^B are product states on each of the two hilbert spaces.

If however ρ^{AB} does not admit to a decomposition on the form (8) it is called an *entangled* state. The most commonly occuring entangled states are the four two-qubit Bell states.

$$\begin{aligned} |\phi^+\rangle &= \frac{1}{\sqrt{2}}\left(|00\rangle + |11\rangle\right) \qquad |\phi^-\rangle = \frac{1}{\sqrt{2}}\left(|00\rangle - |11\rangle\right) \\ |\psi^+\rangle &= \frac{1}{\sqrt{2}}\left(|01\rangle + |10\rangle\right) \qquad |\psi^-\rangle = \frac{1}{\sqrt{2}}\left(|01\rangle - |10\rangle\right) \end{aligned} \tag{9}$$

What happens when you study the reduced state ρ^A of an entangled state? Calculating the partial trace of a Bell state, say $|\phi^+\rangle$:

$$\rho^A = \frac{1}{2}\sum_{i=0,1} \langle i| \left(|00\rangle + |11\rangle\right)\left(\langle 00| + \langle 11|\right)|i\rangle = \frac{1}{2}\left(|0\rangle\langle 0| + |1\rangle\langle 1|\right) \tag{10}$$

The reduced state of the maximally entangled state $|\phi^+\rangle$ is maximally mixed. This implies that it is not possible to associate this subsystem to a state vector and emphasizes the inability to understand one subsystem without the other. Such a phenomenon as entangled states has no counterpart in classical physics.

2.4 CHSH-inequality

The most elementary case of a non-trivial Bell inequality is the Clauser-Horne-Shimony-Holt (CHSH) inequality considering two parties Alice and Bob each performing one of two possible two outcome measurements A_x and B_y for $x, y = 0, 1$ respectively on a shared state $|\psi\rangle$. Assume that the outcomes of measurements A_0, A_1, B_0, B_1 are labeled ± 1. Consider the expectation value

$$S_{CHSH} = \langle A_0B_0 + A_0B_1 + A_1B_0 - A_1B_1\rangle \tag{11}$$

Assume that Alice and Bob are sharing a hidden variable λ with some distribution function $q(\lambda)$. In a local realist model obeying the principle of locality the outcome of Alice's measurement is independent of Bob's measurement and therefore the probability distribution factors and each expectation value in (11) can be written

$$\langle A_iB_j\rangle = \int A_i(\lambda)B_j(\lambda)q(\lambda)d\lambda \tag{12}$$

Thus with some rewriting:

$$S_{CHSH} = \int q(\lambda)\Big(\big(B_0(\lambda) + B_1(\lambda)\big)A_0(\lambda) + \big(B_0(\lambda) - B_1(\lambda)\big)A_1(\lambda)\Big)d\lambda \quad (13)$$

There are a few possibilities. Either $B_0 = B_1 = \pm 1$ implying $B_0 + B_1 = \pm 2$ or $B_0 = \pm 1$ and $B_1 = -B_0$ implying $B_0 + B_1 = 0$. Thus the CHSH-inequality is found [31]

$$|S_{CHSH}| \leq \int q(\lambda)\left(|B_0(\lambda) + B_1(\lambda)| + |B_0(\lambda) - B_1(\lambda)|\right) = 2 \quad (14)$$

Any LHV model must satisfy the CHSH-inequality. However quantum mechanics allows for violations of the inequality. The upper bound on probability distributions with a quantum model is given by Cirel'son's bound stating that if Alice and Bob perform local measurements on a maximally entangled quantum state then $2\sqrt{2}$ constitutes an upper bound of S_{CHSH} [32]. We show this by assuming the existence of a quantum model of the probability distribution $p(a, b|x, z)$ where a, b are the outcomes of Alice and Bob respectively. When considering the quantity S_{CHSH} the expectation values can in a quantum mechanical framework be written

$$\langle A_i B_j \rangle = \langle \psi | A_i \otimes B_j | \psi \rangle \quad (15)$$

for some state $|\psi\rangle$. For simplicity introduce vectors corresponding to Alice and Bob respectively making a measurement on the shared pure state.

$$|\alpha_i\rangle = A_i \otimes \mathbf{1}|\psi\rangle \quad (16)$$

$$|\beta_j\rangle = \mathbf{1} \otimes B_j|\psi\rangle \quad (17)$$

Rewrite S_{CHSH} and find an upper bound

$$S_{CHSH} = \langle \alpha_0| \left(|\beta_0\rangle + |\beta_1\rangle\right) + \langle \alpha_1| \left(|\beta_0\rangle - |\beta_1\rangle\right) \leq \||\beta_0\rangle + |\beta_1\rangle\| + \||\beta_0\rangle - |\beta_1\rangle\| \quad (18)$$

Introduce the notation $\cos(\phi) = |\langle \beta_0|\beta_1\rangle|$. Then the upper CHSH-bound on a quantum probability distribution is

$$S_{CHSH} \leq \sqrt{2|1 + \cos(\phi)|} + \sqrt{2|1 - \cos(\phi)|} = 2\left(\cos\left(\frac{\phi}{2}\right) + \sin\left(\frac{\phi}{2}\right)\right) \quad (19)$$

The right hand side reaches a maximum value for $\phi = \frac{\pi}{2}$ yielding

$$|S_{CHSH}| \leq 2\sqrt{2} \quad (20)$$

In conclusion the CHSH-inequality can discriminate between classically attainable and quantumly attainable correlations.

2.5 GHZ-paradox

To show that particular quantum correlations are nonlocal, it is sufficient to show that there exists a Bell inequality that is violated. However there are other methods of demonstrating nonlocality than explicitly constructing inequalities (although these can always be written as inequalities). The Greenberger-Horne-Zeilinger (GHZ) paradox may be the most famous example where some clever (and surprisingly simple) logical arguments can show contradictions between local models and quantum mechanics.

Introduce three players Alice, Bob and Charlie. Each player is given two possible inputs $x, y, z = 0, 1$ respectively. Given an input, a player yields a corresponding output $A_x, B_y, C_z = \pm 1$. Assume that Alice, Bob and Charlie share a three-partite GHZ-state defined as

$$|GHZ\rangle = \frac{|000\rangle + |111\rangle}{\sqrt{2}} \tag{21}$$

and that the inputs of each party are associated to the Pauli measurements σ_x and σ_y. Then it is easy to see the following four relation hold true

$$\begin{aligned} A_0 B_0 C_0 &= 1 \\ A_0 B_1 C_1 &= -1 \\ A_1 B_0 C_1 &= -1 \\ A_1 B_1 C_0 &= -1 \end{aligned} \tag{22}$$

These quantum predictions should be compared to those of a local model where each input together with a hidden variable λ deterministically gives and outcome ± 1. Hence all outcomes associated to the same measurement are the same. This is in direct contradiction with (22) and it becomes obvious if the product of all left hand sides is compared to the product of all right hand sides. The left hand side product is 1 while the right hand side product is -1 and thus a contradiction with local models is found [34].

In multipartite systems, the GHZ-states are the states whose quantum behavior is most well understood. They are sometimes referred to as 'extremely non-classical'. The GHZ-states constitute the states that can be used to yield intersection points between the quantum and no-signaling[3] polytopes in Bell

[3] The no-signaling principle is a profound principle of quantum information theory stating two parties cannot signal their inputs in order to obtain stronger correlations i.e., that the input of one party cannot affect the outcome of another party.

scenarios. Their properties have been studied using the Mermin inequality for multipartite Bell scenarios [35].

3 Bell inequalities

In this section we will introduce star-networks more rigorously and present four Bell-inequalities regarding various such networks.

3.1 Definitions

This section provides and defines the most fundamental concepts of this thesis. The concepts mentioned in the introduction will here be given a rigorous mathematical framework adapted to the star-network configuration.

Definition 1:(Multipartite star-network measurement scenario). An L-partite star-network measurement scenario with n sources is defined as $(L-1)\times n$ parties called edge parties where the n groups of $L-1$ parties associated to a unique source share hidden variables. All edge parties share one hidden variable with a center party labeled Bob. Each of the $(L-1)\times n$ edge parties can locally perform one of $M \in \mathbb{N}_+$ measurements on their part of the respective L-qudit states with each measurement having d possible outcomes. Bob is free to locally perform any number of measurements on any part of the state at his disposal.

When working with bipartite star-networks with many sources we will be using the following notations: Each of the n edge parties is referred to as party i for $i \in \mathbb{N}_n$. The measurement performed by party i is denoted $m_i \in \{0, 1, \ldots, M-1\}$. The corresponding outcome of party i is denoted $r_i \in \{0, 1, \ldots, d-1\}$. Bob's measurement is denoted $y \in \{0, 1, \ldots, M_{Bob}-1\}$ and the corresponding outcome is labeled b.

Although when we work with three party star-networks we prefer alternative notations: the three parties will be called Alice, Bob and Charlie. The measurement of Alice is denoted $x \in \{0, 1, \ldots, M-1\}$ and similarly Charlie's measurement is denoted $z \in \{0, 1, \ldots, M-1\}$. The corresponding outcomes are denoted $a \in \{0, 1, \ldots, d-1\}$ and $c \in \{0, 1, \ldots, d-1\}$ respectively.

Definition 2:. (Star-network LHV model). An LHV model for an L-partite star-network measurement scenario with n sources is defined by a set of functions $\{f_i^j\}$ where $i = 1, ..., n$ and $j = 1, ..., L-1$ such that $f_i^j : \Lambda_i \times \mathbb{Z}_{M-1} \to \mathbb{Z}_{d-1}$ where each Λ_i for $i = 1, 2, \ldots, n$ is a set to which a distribution q_i is associated, and a function for Bob, $f_{Bob} : \Lambda_1 \times \ldots \times \Lambda_n \times \mathbb{Z}_y \to \mathbb{Z}_{d^n}$.

Due to the determinism built into LHVs one may assign a set of hidden variables $\lambda_i \in \Lambda_i$ shared between the edge parties associated to source i and Bob such that the outcome of any edge party with access to hidden variable from source i is completely determined by the measurement and the hidden variable λ_i.

We now introduce the central definition of this thesis. Any LHV model for a bipartite star-network measurement scenario with n sources centered about Bob is subject to an assumption of local realism as follows

$$P(r_1, ..., r_n, b|m_1, ..., m_n, y) = \int q(\lambda) P(b|y, \lambda) \prod_{i=1}^{n} P(r_i|m_i, \lambda_i) d\overline{\lambda} \tag{23}$$

We call (23) the n-local assumption. For convenience we will frequently use $\overline{\lambda} = (\lambda_1, ..., \lambda_n)$. The postulate (23) enforces realism through the hidden variables as given in definition 2 effectively mapping each probability involved either to zero or to unity. The n-local assumption also captures the fact that locality enforces the probability distribution of each party in the network to be independent of the outcomes of the other parties. In addition, we need to enforce that all sources are indepdent of each other implying that the probability density function $q(\lambda)$ allows for factoring:

$$q(\lambda) = \prod_{i=1}^{n} q_i(\lambda_i) \tag{24}$$

If a conditional probability distribution $P(r_1, ..., r_n, b|m_1, ..., m_n, y)$ can be written on the form (23) obeying (24) there exist an LHV description and the probability distribution is termed n-local. Otherwise we say that the distribution is non n-local. See figure 2 for an example of a star-network measurement scenario under the 3-local assumption.

The possibility of making local measurements on entangled states enables the existence of nonlocal correlations in quantum mechanics. We repeat a standard definition in literature:

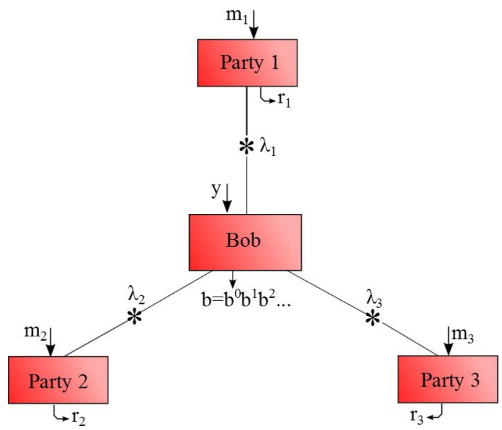

Figure 2: $n = 3$ bipartite star-network measurement scenario with hidden variable distribution as assumed under the 3-local assumption.

Definition 4:(qubit correlation function). A correlation function for two parties performing one of two possible two-outcome measurements is defined as

$$\langle A_x C_z \rangle = \sum_{a,c=0,1} (-1)^{a+c} P(a,c|x,z) \tag{25}$$

If Alice obtaining the result a ($\bar{a}$) implies Charlie obtaining $c = a$ ($\bar{c} = \bar{a}$) then we say that Alice and Charlie are perfectly correlated yielding $\langle A_x C_z \rangle = 1$. If however Alice obtaining a implies $c = \bar{a}$ where the bar denotes a 'logical not operation' then we say that Alice and Charlie are perfectly anti-correlated yielding $\langle A_x C_z \rangle = -1$.

The definition of two-party qubit correlation function is intuitive, however the notion of correlation and how to quantify it is not obvious when considering systems of dimension $d > 2$. As a consequence we introduce a broader definition.

Definition 5: (n-party qudit correlation function). A general correlation function F for n edge parties in a bipartite star-network performing d-outcome measurements is defined as a linear combination of N functions

$$f^{(k)} : r_1 \times r_2 \times ... \times r_n \to \mathbb{C} \tag{26}$$

for $\forall k \in \mathbb{N}_N$ such that $i)$ $f^{(k)}(r_1, \ldots, r_n) = f_1^{(k)}(r_1) f_2^{(k)}(r_2) \ldots f_n^{(k)}(r_n)$, $ii)$ $|f_i^{(k)}(*)| \leq 1$ for all $i \in \mathbb{N}_n$, $iii)$ $f^{(k)}$ is linear in all variables and $iv)$ F is completely symmetric under any permutation of the outputs of the edge parties.

3.2 Bipartite inequalities $2 \to 2$

We are now ready to provide novel Bell inequalities. In this section we consider the scenario of an bipartite star-network of n sources centered about Bob performing one of 2 measurements with two possible outcomes. It will referred to as the $2 \to 2$ inequality. The measurements of Bob are evidently not complete measurements but partial measurements corresponding to grouping the set of outcomes into two distinguishable sets. In general such partial measurements are realized with a set of POVMs.

Preferably, one would be more interested in a complete measurement for Bob. The reason that we begin by considering the Bob $2 \to 2$ case is that it has been shown that a complete Bell state measurement in photonics cannot be experimentally realized using linear optics [36]. Thus the Bob $2 \to 2$ is initially motivated by experimental limitations in linear optics experiments.

Start by introducing correlators defined from a modified version of the correlation function in definition 4 extended to including n party correlations.

$$\langle B_y C^1_{m_1} C^2_{m_2} ... C^n_{m_n} \rangle = \sum_{b,r_1,...,r_n} (-1)^{b+\sum_{i=1}^n r_i} P(r_1, ..., r_n, b|m_1, ..., m_n, y) \quad (27)$$

Form quantities from linear combinations of the correlators in (27): one symmetric quantity and one anti-symmetric quantity

$$I = \frac{1}{M^n} \sum_{m_1,...,m_n=0}^{M-1} \langle B_0 C^1_{m_1} C^2_{m_2} ... C^n_{m_n} \rangle \quad (28)$$

$$J = \frac{1}{M^n} \sum_{m_1,...,m_n=0}^{M-1} (\omega)^{\sum_{i=1}^n m_i} \langle B_1 C^1_{m_1} C^2_{m_2} ... C^n_{m_n} \rangle \quad (29)$$

where $\omega = \exp\left(\frac{2\pi i}{M}\right)$ is the root of unity. Observe that we provide an arbitrary number of measurements M for the edge parties.

Now we state and prove the first general result:

Theorem 1: (Bob $2 \to 2$ qubit bipartite n-locality). If a probability distribution $P(b, r_1, \ldots, r_n | y, m_1, \ldots, m_n)$ corresponding to a bipartite star-network with n sources where $y \in \{0, 1\}$ and $d = 2$, is n-local then it must satisfy the inequality

$$S^{2\to2}(n) \equiv |I|^{1/n} + |J|^{1/n} \leq 1 \tag{30}$$

Proof:

Start with considering only the quantity I, by (27,28):

$$I = \frac{1}{M^n} \sum_{m_1,...,m_n} \sum_{b,r_1,...,r_n} (-1)^{b+\sum_{i=1}^n r_i} P(b, r_1, ..., r_n | y = 0, m_1, ..., m_n) \tag{31}$$

Implement the n-locality assumption (23,24)

$$I = \frac{1}{M^n} \sum_{m_1,...,m_n} \sum_{b,r_1,...,r_n} (-1)^{b+\sum_{i=1}^n r_i} \int q(\lambda) P(b|y = 0, \lambda) \prod_{i=1}^n P(r_i | m_i, \lambda_i) d\lambda_i \tag{32}$$

Group terms by factors and split the sum over $b, r_1, r_2, .., r_n$

$$I = \frac{1}{M^n} \sum_{m_1,...,m_n} \int q(\lambda) \sum_b (-1)^b P(b|y = 0, \lambda) \prod_{i=1}^n \sum_{r_i=0,1} (-1)^{r_i} P(r_i | m_i, \lambda_i) d\lambda_i \tag{33}$$

This constitutes a local realist expression for I. Introduce new correlators constructed from this expression conditioned on the hidden variables

$$\langle C^i_{m_i} \rangle_{\lambda_i} = \sum_{r_i=0,1} (-1)^{r_i} P(r_i | m_i, \lambda_i) \tag{34}$$

$$\langle B_y \rangle_{\lambda_1,...,\lambda_n} = \sum_b (-1)^b P(b|y, \lambda) \tag{35}$$

With these new correlators I takes the form

$$I = \frac{1}{M^n} \sum_{m_1,...,m_n=0}^{M-1} \int q(\lambda) \langle B_0 \rangle_\lambda \prod_{i=1}^n \langle C^i_{m_i} \rangle_{\lambda_i} d\lambda_i \tag{36}$$

Only the product series over the correlators $\langle C^i_{m_i} \rangle_{\lambda_i}$ depends on the measurements. In (36) we may interchange summation and product series. We will not give the proof here but it can be justified using induction.

$$\sum_{m_1,\ldots,m_n=0}^{M-1} \prod_{i=1}^{n} \langle C^i_{m_i} \rangle_{\lambda_i} = \prod_{i=1}^{n} \sum_{m_1,\ldots,m_n=0}^{M-1} \langle C^i_{m_i} \rangle_{\lambda_i} \tag{37}$$

Implementing (37) with (36) yields

$$I = \frac{1}{M^n} \int q(\lambda) \langle B_0 \rangle_{\lambda_1,\ldots,\lambda_n} \prod_{i=1}^{n} \sum_{m_i=0}^{M-1} \langle C^i_{m_i} \rangle_{\lambda_i} d\lambda_i \tag{38}$$

From the n-local assumption it is imposed that the probability density function factors. Estimate an upper bound as follows

$$|I| \leq \frac{1}{M^n} \int \prod_{i=1}^{n} \left| \sum_{m_i=0}^{M-1} \langle C^i_{m_i} \rangle_{\lambda_i} \right| q_i(\lambda_i) d\lambda_i \tag{39}$$

Observe that we have eliminated $\langle B_0 \rangle_{\overline{\lambda}}$ since it is bounded by a modulus of unity. We are left with an expression (39) that is a product of independent variables and hence allows for a factorization

$$|I| \leq \prod_{i=1}^{n} \int q_i(\lambda_i) \frac{1}{M} \left| \sum_{m_i=0}^{M-1} \langle C^i_{m_i} \rangle_{\lambda_i} \right| d\lambda_i \tag{40}$$

An analog analysis for the quantity J yields

$$|J| \leq \prod_{i=1}^{n} \int q_i(\lambda_i) \frac{1}{M} \left| \sum_{m_i=0}^{M-1} \omega^{m_i} \langle C^i_{m_i} \rangle_{\lambda_i} \right| d\lambda_i \tag{41}$$

Introduce notations as follows:

$$x_i = \int q_i(\lambda_i) \frac{1}{M} \left| \sum_{m_1=0}^{M-1} \langle C^i_{m_i} \rangle_{\lambda_i} \right| d\lambda_i \tag{42}$$

$$y_i = \int q_i(\lambda_i) \frac{1}{M} \left| \sum_{m_1=0}^{M-1} \omega^{m_i} \langle C^i_{m_i} \rangle_{\lambda_i} \right| d\lambda_i \tag{43}$$

Implementing the new notation

$$|I| \leq x_1 x_2 \ldots x_n \qquad |J| \leq y_1 y_2 \ldots y_n \tag{44}$$

In order to proceed lemma 1 is derived (see appendix A) and applied.

$$|I|^{1/n} + |J|^{1/n} \leq \prod_{i=1}^{n} (x_i + y_i)^{1/n} =$$

$$\left(\prod_{i=1}^{n} \int q_i(\lambda_i) \frac{1}{M} \left(\left| \sum_{m_i=0}^{M-1} \langle C^i_{m_i} \rangle_{\lambda_i} \right| + \left| \sum_{m_i=0}^{M-1} \omega^{m_i} \langle C^i_{m_i} \rangle_{\lambda_i} \right| \right) d\lambda_i \right)^{1/n} \tag{45}$$

Since the correlators in (34,35) are real, bounded by modulus unity and can in principle be chosen independently of each other, we provide the estimation

$$\left| \sum_{m_1,\ldots,m_n=0}^{M-1} \langle C^i_{m_i} \rangle_{\lambda_i} \right| + \left| \sum_{m_1,\ldots,m_n=0}^{M-1} \omega^{\sum_{i=1}^{n} m_i} \langle C^i_{m_i} \rangle_{\lambda_i} \right| \leq M \tag{46}$$

This is an optimization over a hypercube in the space of the quantities (34). Implementing (46) we obtain

$$|I|^{1/n} + |J|^{1/n} \leq \left(\prod_{i=1}^{n} \int q_i(\lambda_i) d\lambda_i \right)^{1/n} \tag{47}$$

Every $q_i(\lambda_i)$ is a probability density function and therefore

$$|I|^{1/n} + |J|^{1/n} \leq 1 \tag{48}$$

This concludes the proof.

■

Theorem 1 is a one way theorem. It should not be too difficult to study whether it holds that $P(b, r_1, r_2, \ldots, r_n | y, m_1, m_2, \ldots, m_n)$ is n-local if and only if it satisfies inequality (30). In section 3.4 we will show that this is in fact is true.

As it comes to bipartite $2 \to 2$ inequalities we also demonstrate how to construct a Bell inequality for star-networks where the n sources are emitting qutrits and the edge parties perform three-outcome measurements. The construction of such an inequality is not difficult since it is a slight modification of theorem 1. However the inequality is only interesting (non-trivial) if it can be violated by quantum mechanics. As it turns out, the construction of a quantum mechanically non-trivial qutrit n-locality inequality is a much more difficult task, by intuition because the geometry of the n-local set becomes more complex. The inequality presented here is the only example observed so far of such a non-trivial inequality but it is probably the case that stronger inequalities can in principle be constructed. In order for the inequality to be non-trivial we enforce three choices of measurements for the edge parties. The modifications needed from theorem 1 is that the outputs of the edge parties are mapped onto the three roots of unity $1, \omega^{\frac{2\pi i}{3}}, \omega^{\frac{4\pi i}{3}}$. The corresponding I, J would be

$$I_3 = \frac{1}{9} \sum_{\overline{m}, \overline{r}} \omega^{a+b+c} P(a, b, c|x, z) \tag{49}$$

$$J_3 = \frac{1}{9} \sum_{\overline{m}, \overline{r}} \omega^{a+b+c+x+z} P(a, b, c|x, z) \tag{50}$$

The process of obtaining an inequality is analog to theorem 1 with exception of putting the upper bound on the LHV correlations. Following the outline of theorem 1, the analog of the upper bound in equation (46) will be

$$\frac{1}{3}\left(\left|\langle C_0^i \rangle_{\lambda_i} + \langle C_1^i \rangle_{\lambda_i} + \langle C_2^i \rangle_{\lambda_i}\right| + \left|\langle C_0^i \rangle_{\lambda_i} + \omega \langle C_1^i \rangle_{\lambda_i} + \omega^2 \langle C_2^i \rangle_{\lambda_i}\right|\right) \leq \frac{2}{\sqrt{3}} \tag{51}$$

where the quantities $\langle C_{m_i}^i \rangle_{\lambda_i}$, in analogy with (34), are convex combinations of the roots of unity with probability weights. The upper bound in (51) is obtained optimizing over the convex hull of the three roots of unity in the complex plane. The final inequality will be

$$|I_3|^{1/n} + |J_3|^{1/n} \leq \frac{2}{\sqrt{3}} \tag{52}$$

The fact that (52) is non-trivial will be demonstrated in section 4.1.

3.3 Bipartite inequality $1 \to 2^n$

While the relevance of the previous section is motivated by experimental limitations, the analog bipartite star-network measurement scenario of n sources with Bob always performing a fixed measurement on the n qubits at his disposal and obtaining one of 2^n possible outcomes (complete measurement), is the more intuitive scenario. Bob's measurement will typically be chosen as a complete Bell state measurement since such a measurement has been shown to generate quantum correlations in various quantum information applications such as teleportation. It is simply a reasonable guess.

The scenario considered in this section is labeled $1 \to 2^n$. Define the same correlators as in (27) but with a slight modification

$$\langle B^i C^1_{m_1} ... C^n_{m_n} \rangle = \sum_{b^1 ... b^n r_1, ..., r_n} (-1)^{\sum_{i=1}^n r_i} f_i(b) P(b^1 ... b^n, r_1, ..., r_n | m_1, ..., m_n) \tag{53}$$

where $|f_i(b)| \leq 1$ is some arbitrary function of the bitstring b. Using the correlation function in (53) introduce quantities Q_1, Q_2 formed by linear combinations of correlators:

$$Q_1 = \frac{1}{M^n} \sum_{m_1, ..., m_n} \langle B C^1_{m_1} ... C^n_{m_n} \rangle$$

$$Q_2 = \frac{1}{M^n} \sum_{m_1, ..., m_n} \omega^{\sum_{i=1}^n m_i} \langle B C^1_{m_1} ... C^n_{m_n} \rangle \tag{54}$$

This is highly reminiscent of the $2 \to 2$ case but with the difference that the two quantities in (54) are strongly coupled in comparison to the partial measurement scenario since they are both generated by the same measurement of Bob.

Theorem 2: ($1 \to 2^n$ qubit bipartite n-locality). If a probability distribution $P(b^1 b^2 \ldots b^n, r_1, r_2, \ldots, r_n | m_1, m_2, \ldots, m_n)$ corresponding to a bipartite star-network measurement scenario of n sources with $d = 2$ where Bob performs a fixed complete measurement is n-local it satisfies the inequality

$$S^{1 \to 2^n}(n) = |Q_1|^{1/n} + |Q_2|^{1/n} \leq 1 \tag{55}$$

Proof:

The proof for inequality (55) is analogous to the proof method of theorem 1 and will not be shown explicitly.

■

An important feature of the $1 \to 2^n$ inequality is that the results of [33] constitute a special case of (55), namely the inequality corresponding to $n = 2$.

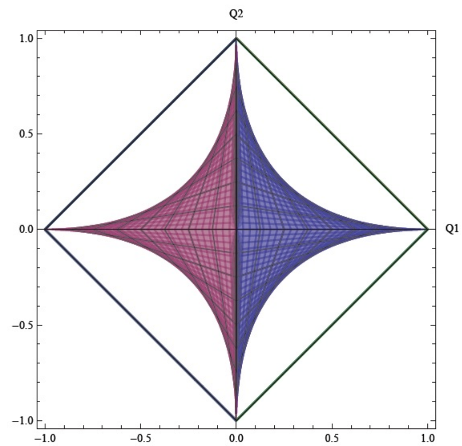

Figure 3: The bilocal set of probability distributions corresponding to a bipartite $n = 2$ star-network measurement scenario. The thick black line enclosing the bilocal set is the boundary of the local set arising in Bell measurement scenarios.

Remark: one could raise an issue of with the quantities used to derive the inequality. Evidently if $n > 2$ there exists no correlator and quantity that is conditioned on $b^3, .., b^n$ which may or may not constrain the results achievable with a quantum model. One could argue that n quantities Q_i each conditioned on a bit in the bitstring output of Bob would be necessary. This was also the initial form of the derived inequality of which inequality (55) constitutes a special case but after extensive studies it was shown that such an inequality can, without loss of generalization, be reduced to the inequality presented in theorem 2. We will not take the reader through such a detour.

3.4 Structure of the n-local set

As is the case with theorem 1, theorem 2 is a one way theorem. A necessary but not sufficient criteria for knowing if (55) is a 'good' inequality or not is whether there exists an LHV yielding equality in (55) i.e., there exists a an n-local probability distribution realizing $S^{1\to 2^n} = 1$. A much stronger criteria is whether the lower quantum bound predicted by the inequality continuously coincides with the upper classical bound realizable with a family of LHVs i.e., the inequality is tight. We illustrate this bound in figure 3 for bilocal ($n = 2$) probability distributions detected by the inequality in (55). By comparison to the thicker line enclosing the fully deterministic points of the predicted bilocal set representing the set of local correlations from an ordinary Bell scenario it is evident that the bilocal assumption is significantly stronger constraint than Bell's assumption of local causality. Thus, a probability distribution violating bilocality, or by extension n-locality may be locally attainable in a Bell scenario due to the possibility of sharing randomness that is not possible in entanglement swapping.

We now show that inequality (55) properly characterizes the boundaries of the n-local set. This proof directly extends to include inequality (30).

Theorem 3: (n-local set boundaries). For each Q_1 and Q_2 satisfying inequality (55) there exists an n-local probability distribution $P(b^1b^2 \dots b^n, r_1, r_2, \dots, r_n | m_1, m_2, \dots, m_n)$ corresponding to a bipartite star-network measurement scenario of n sources with $M = d = 2$ that achieves the values of Q_1 and Q_2.

Proof:

We start by showing that there exists an LHV model that realizes the upper bound in (55) once given a value of n.

Let the hidden variable shared between party i and Bob be λ_i for $i = 1, \dots, n$. As the correlation function is defined in equation (54) the condition

$$r_1 \oplus \dots \oplus r_n \oplus b^y = 0 \tag{56}$$

must be satisfied in order to maximize the symmetric quantity Q_1. An LHV performing this task is

$$r_i = \lambda_i \quad b^{1,2,\dots,n} = \bigoplus_{i=1}^{n} \lambda_i \tag{57}$$

Thus this LHV implies that $Q_1 = 1$. It follows from theorem 2 that the antisymmetric quantity $Q_2 = 0$. The LHV (57) satisfies the upper bound of inequality (55) for all values of n. In figure 3 this strategy, for $n = 2$, realizes the bilocal point $(1, 0)$.

Similarly, in order to find an optimal n-local strategy maximizing the antisymmetric quantity Q_2 the following condition must be satisfied due to the introduced correlation function, see (54).

$$b^y \oplus \bigoplus_{i=1}^{n} (r_i \oplus m_i) = 0 \tag{58}$$

An LHV performing this task is

$$r_i = m_i + \lambda_i \qquad b^{1,2,\ldots,n} = \bigoplus_{i=1}^{n} \lambda_i \tag{59}$$

It is evident that the strategy (59) yielding $Q_2 = 1$ implies $Q_1 = 0$ under the constraint of theorem 2. For the special case of $n = 2$ this corresponds to the point $(0, 1)$ in figure 3.

The intension is now to mix strategies to explore the trade off. Introduce a string of binary random variables $u = u_1 ... u_n$ with $u_i \in \{0, 1\}$ and construct a new LHV such that

$$r_i = \lambda_i \oplus u_i m_i \qquad b^{1,2,\ldots,n} = \bigoplus_{i=1}^{n} \lambda_i \tag{60}$$

For each possible value of the random variables in the bitstring u there is a corresponding value of quantities (Q_1, Q_2). The all-zero bitstring $u = 0$ returns the optimal strategy for the symmetric quantity Q_1 while the all-one bitstring $u = 1$ returns the optimal strategy for the antisymmetric quantity Q_2. Any other u implies $Q_1 = Q_2 = 0$ due to the no-signaling principle. The random variables are each subject to a distribution P_i. Enforcing the n-local assumption on the distributions:

$$P(u) = \prod_{i=1}^{n} P_i(u_i) \tag{61}$$

Let $P_i(u_i = 0) = p_i$, then

$$P_i(u_i) = (p_i, 1 - p_i) \tag{62}$$

for $i = 1, 2, ..., n$. Since only two bitstrings u contribute to the quantities Q_1, Q_2

$$(Q_1, Q_2) = \prod_{i=1}^{n} p_i \,(1, 0) + \prod_{i=1}^{n} (1 - p_i)\,(0, 1) \tag{63}$$

Even though we are working only with non-negative (Q_1, Q_2), analog arguments will hold also in other quadrants in the Q_1Q_2-plane. This provides a bounded closed simply connected set. We need now only to characterize the boundary of this set.

Enforce symmetry in the distribution of random variables by letting $p_i = p \ \forall i \in \mathbb{N}_n$. Then (63) becomes

$$Q_1 = p^n \quad Q_2 = (1-p)^n \tag{64}$$

Thus for all $p \in [0,1]$ the upper bound of inequality (55) is realized.

$$|Q_1|^{1/n} + |Q_2|^{1/n} = 1 \tag{65}$$

Hence the upper LHV bound of the n-local set predicted by inequality (55) is continuously realizable with LHV models and thus shows tightness of the inequality.

■

This analysis provides a proper physical understanding and characterization of the general n-local set. It is clear that the trade-off between the two deterministic points $(Q_1, Q_2) = (1, 0)$ and $(Q_1, Q_2) = (0, 1)$ yields the non-convex structure of the n-local set. Evidently the n-local set is not a polytope as is the local set in Bell scenarios (see figure 3), but a more complicated object.

As a remark one can prove theorem 3 with other methods than mixing between LHV strategies. An example of an alternative proof is performing a direct n-local decomposition as described in the definition of n-locality and under the assumption of uniform marginal probability distribution one can derive a result equivalent to that of theorem 3. Despite this certainly being more elegant than the proof of theorem 3, we do not need to present the alternative proof.

3.5 Multipartite inequality

So far we have only considered star-networks with bipartite sources. We will generalize this to L-partite sources (explained in definition 1) in this section. Thus we are concerned with the most general class of star-networks involving qubit distribution. See figure 4 for an illustration of a $L = 3$ star-network.

For each of the n sources we associate $L-1$ edge parties. From the n sources of $L-1$ edge parties each, we form $L-1$ groups consisting of n parties in such a way that there are no two parties in the same group that share a hidden variable. We label these groups by an index $k = 1, ..., L-1$. Furthermore we arrange the order within in each group such that party number j in each group shares randomness with all parties of index j in the other $L-2$ groups. As an example, in figure 4 such groups would be Alice/Charlie and Albert/Carol. Each edge party makes a measurement labeled m_j^k. The corresponding outcomes are labeled r_j^k. We use $\overline{m}$ to denote the string of all measurements $\overline{r}$ for the string of all outcomes.

Crucially we need to extend the definition of n-local probability distributions to include the L-partite case. This is easily done along the lines of (23,24)

$$P(\overline{r}, b|\overline{m}, y) = \int \prod_{i=1}^{n} q_i(\lambda_i) P(b|\overline{\lambda}, y) \prod_{k=1}^{L-1} \prod_{j=1}^{n} P(r_j^k|m_j^k, \lambda_j) d\overline{\lambda} \tag{66}$$

We show how to generalize the n-locality inequality (30) to the corresponding L-partite case. Introduce a set of 2^{L-1} quantities of linear combinations of conditional probabilities. The set of quantities is $\{K_X\}$ where we let X run over all subsets of $\mathbb{N}_{L-1}$ (including the empty set)[4].

$$K_X = \frac{1}{2^{n(L-1)}} \sum_{\overline{m}} g(X) \sum_{\overline{r}} (-1)^{b+\sum_{j,k} r_j^k} P(\overline{r}, b|\overline{m}, y_X) \tag{67}$$

The expression y_X just signifies that the measurement of Bob associated to the set X can be freely chosen. Thus we have the freedom of choosing up to 2^{L-1} measurements for Bob each associated to a different K_X. The function $g(X)$ associates a factor of symmetry or antisymmetry to the linear combination with respect to the measurements of some of the groups k. Explicitly we define $g(X)$

$$g(X) = \prod_{k \in X} (-1)^{\sum_{j=1}^{n} m_j^k} \tag{68}$$

Having introduced these quantities, a legitimate question is: Why do we choose these quantities in particular? Because it is crucial to make a clever

[4] In our convention we do not include zero in the set of natural numbers.

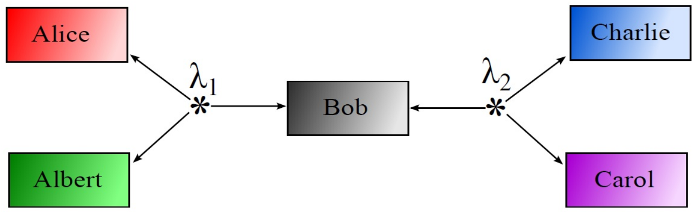

Figure 4: Three-partite bilocality scenario.

choice of quantities in order to uphold interesting quantum mechanical properties of the inequalities and as we will see in section 4.1, these quantities do uphold such interesting properties. However this does not mean that there is no other set of quantities that also may uphold interesting quantum properties.

As it comes to the local realist correlations, we can now state and prove the following generalization of theorem 1

Theorem 4: (L-partite n-locality). If a probability distribution $P(\overline{r}, b|\overline{m}, y)$ corresponding to a L-partite star-network measurement scenario involving n sources with $M = d = 2$ is n-local, then it satisfies the inequality

$$S^{2^{L-1}\to 2}(n, L) \equiv \sum_{X\subset\mathbb{N}_{L-1}} |K_X|^{1/n} \leq 1 \tag{69}$$

Proof:

Introduce the generalized n-local assumption (66) to the quantities (67). Some regrouping of sums will yield for quantity K_X

$$K_X = \frac{1}{2^{n(L-1)}} \sum_{\overline{m}} g(X) \int \prod_{i=1}^{n} q_i(\lambda_i) \sum_b (-1)^b P(b|\overline{\lambda}, y_X) \prod_{k=1}^{L-1} \prod_{j=1}^{n} \sum_{r_j^k} (-1)^{r_j^k} P(r_j^k|m_j^k, \lambda_j) d\overline{\lambda} \tag{70}$$

Perform a relabeling of the sums as

$$\langle B_{y_X}\rangle_{\overline{\lambda}} = \sum_b (-1)^b P(b|\overline{\lambda}, y_X) \tag{71}$$

$$\langle A^{k,j}_{m_j^k}\rangle_{\lambda_j} = \sum_{r_j^k} (-1)^{r_j^k} P(r_j^k|m_j^k, \lambda_j) \tag{72}$$

In the spirit of equations (34-40) it can be shown that

$$|K_X| \leq \frac{1}{2^{n(L-1)}} \prod_{j=1}^{n} \int \prod_{k=1}^{L-1} q_j(\lambda_j) \left| \sum_{m_j^k=0}^{M-1} g_j^k(X) \langle A^{k,j}_{m_j^k} \rangle_{\lambda_j} \right| d\overline{\lambda} \tag{73}$$

where the function $g_j^k(X)$ is a factor of $g(X)$ such that if $k \in X$ we impose the antisymmetrization

$$g_j^k(X) = (-1)^{m_j^k} \tag{74}$$

otherwise $g_j^k(X) = 1$. Also, observe the right hand side expression in (73) is factorable in terms of the hidden variables since we have dropped the quantity $\langle B_{y_X} \rangle_{\overline{\lambda}}$ with the motivation that is bounded by a modulus of unity.

Using lemma 1 (in appendix A) to the set of quantities $\{K_X\}$ yields

$$\sum_{X \subset \mathbb{N}_{L-1}} |K_X|^{1/n} \leq \left(\prod_{j=1}^{n} \int q_j(\lambda_j) \frac{1}{2^{L-1}} \sum_{X \subset \mathbb{N}_{L-1}} \prod_{k=1}^{L-1} \left| \sum_{m_j^k=0}^{M-1} g_j^k(X) \langle A^{k,j}_{m_j^k} \rangle_{\lambda_j} \right| d\lambda_j \right)^{1/n} \tag{75}$$

The problem is reduced to providing a good estimation of the integrand. Fortunately this is easier than it might seem at first sight:

$$\sum_{X \subset \mathbb{N}_{L-1}} \prod_{k=1}^{L-1} \left| \sum_{m_j^k=0}^{M-1} g_j^k(X) \langle A^{k,j}_{m_j^k} \rangle_{\lambda_j} \right| \leq 2^{L-1} \tag{76}$$

The reason for this is that since all the quantities $\langle A^{k,j}_{m_j^k} \rangle_{\lambda_j}$ are real and bounded by a modulus of 1 we are effectively optimizing the left hand side of (76) over a hypercube. This is a closed compact and convex set and it is easy to realize that the optimum of (76) is found at a vertex of the set. However due to the symmetry imposed by the choice of the quantities K_X all vertices of the convex set yield the same value for (76) since optimizing one of the product-quantities in the sum minimizes the modulus of all other quantities. Thus we are reduced to $L-1$ factors that are all optimized and therefore each equal 2. Hence we obtain the upper bound presented.

It is now straightforward to find the inequality. Since q_j for $j = 1, ..., n$ are probability density functions, the integral after factoring out the integrand using estimation (76) is unity. This yields the final inequality

$$\sum_{X \subset \mathbb{N}_{L-1}} |K_X|^{1/n} \leq 1 \tag{77}$$

■

We have now provided an L-partite generalized n-locality inequality. Observe that inequality (30) is a special case of (69) corresponding to $L = 2$ and that the quantities K_X for will be equal to the I, J up to the number of measurements which is here restricted to 2. It is easy to see that we can generalize (69) to include many measurements, the main problem arises from putting a tight upper bound on the expression corresponding to (76) which will no longer be subject to the simple argument we applied for $M = 2$.

3.6 Freedom-of-choice loophole

When deriving Bell inequalities (not only restricted to star-networks) there are various assumptions that need justification. Similarly in experimental test of Bell inequalities there are other assumptions that need justification. Both the theoretical and experimental assumptions are commonly referred to as loopholes that needs closing. However for our purpose here, we are interested in the theoretical principles of reality rather than the experimental loopholes (although these are the most relevant for technological applications). A theoretical loophole arises our assumption of n-locality namely that we have assumed that all parties involved can effectively act as perfect random number generators, using their free will or some pseudorandom number generator to make a uniformly random choice of measurement settings that is independent from all influences of nature. This is an assumption of freedom-of-choice and it is intimately connected with the metaphysical question of free will and superdeterminism. The loophole arising is that if we cannot show resistance to such superdeterministic assumptions, one could (at least in principle) exploit the loophole to construct a local realist theory reproducing the predictions of quantum mechanics.

In this section we show how to approach the freedom of choice loophole in star-networks. This task has previously been undertaken for ordinary Bell scenarios [33] and further developed in [26]. We apply the methods to considering a wider class of networks from now referred to as *extended star-networks*. An extended star-network is a bipartite star-network of $n+1$

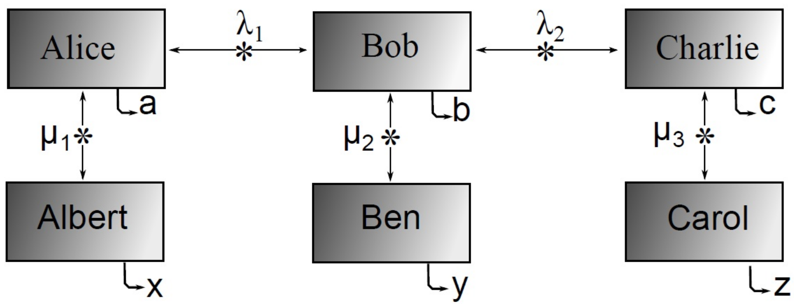

Figure 5: Extended bilocal scenario

parties to which we add $m \leq n+1$ parties such that each of the m parties share randomness with one and only one party in the star-network. An example of an extended star-network for the extended bilocal scenario is displayed in figure 5.

Consider the ordinary bilocality scenario with Alice, Bob and Charlie having inputs x, y, z and outcomes a, b, c respectively. The bilocal assumption going in to our derivation of Bell inequalities reads

$$P_{biloc}(a,b,c|x,y,z) = \int \rho_1(\lambda_1)\rho_2(\lambda_2)P(a|x,\lambda_1)P(b|y,\lambda_1,\lambda_2)P(c|z,\lambda_2)d\lambda_1 d\lambda_2 \tag{78}$$

Quantum mechanics allows us to think of each measurement outcome of each party as a discrete random number generator. However the settings of these random number generators are subject to the freedom-of-choice loophole so we assume that the setting of each random number generator is determined by some hidden variables μ_1, μ_2, μ_3 such in fact all edge parties are subject to superdeterminism and therefore have no free will. The choices of measurements are given by $P(x|\mu_1), P(y|\mu_2), P(z|\mu_3)$ which is always zero or unity. The hidden variables are subject to distributions q_1, q_2, q_3 since these are independent of each other. The distribution (78) now takes the form

$$P_{biloc}(a,b,c,x,y,z) = \int \rho_1(\lambda_1)\rho_2(\lambda_2)q_1(\mu_1)q_2(\mu_2)q_3(\mu_3)P(x|\mu_1)P(y|\mu_2)P(z|\mu_3) \\ P(a|x,\lambda_1)P(b|y,\lambda_1,\lambda_2)P(c|z,\lambda_2)d\overline{\lambda}d\overline{\mu} \tag{79}$$

The bilocal scenario will be put in contrast to the extended bilocal scenario displayed in figure 5. The system involves six parties where no party in the network has any choice of measurement settings i.e., free will nor hidden measurement settings make an observable difference to the system. The outcomes are labeled by a, b, c, x, y, z. A local realist assumption in analogy with the n-local assumption would be

$$P_{ExtBiloc}(a,b,c,x,y,z) = \int \rho_1(\lambda_1)\rho_2(\lambda_2)q_1(\mu_1)q_2(\mu_2)q_3(\mu_3)P(x|\mu_1)P(y|\mu_2)P(z|\mu_3) \\ P(a|\mu_1,\lambda_1)P(b|\mu_2,\lambda_1,\lambda_2)P(c|\mu_3,\lambda_2)d\overline{\lambda}d\overline{\mu} \tag{80}$$

Under the realist assumption and assuming that our measurement do not have trivial outcomes we enforce that $P(x,y) = P(x)P(y) > 0$. We state and prove the following theorem.

Theorem 5:(Freedom-of-choice loophole). The probability distribution $P_{ExtBiloc}$ is extended bilocal if and only if the conditional probability distribution P_{biloc} is bilocal, where we interpret the outcomes x, y, z of the extended bilocality scenario as inputs of the ordinary bilocality scenario.

Proof:

Assume that $P_{ExtBiloc}$ admits to the decomposition (80). Then elementary conditional probability gives us $q_1(\mu_1)P(x|\mu_1) = q_1(\mu_1|x)P(x)$ and similarly for the other two extended parties. Since $P_{ExtBiloc}$ is extended bilocal it follows that

$$P_{ExtBiloc}(a,b,c|x,y,z) = \frac{P_{ExtBiloc}(a,b,c,x,y,z)}{P(x)P(y)P(z)} \tag{81}$$

Carrying out (81) and labeling

$$\begin{aligned} P(a|x,\lambda_1) &= \int q_1(\mu_1|x)P(a|\mu_1,\lambda_1)d\mu_1 \\ P(b|y,\lambda_1,\lambda_2) &= \int q_2(\mu_2|y)P(b|\mu_2,\lambda_1,\lambda_2)d\mu_2 \\ P(a|x,\lambda_1) &= \int q_2(\mu_3|x)P(a|\mu_3,\lambda_2)d\mu_3 \end{aligned} \tag{82}$$

brings $P_{ExtBiloc}$ to the form

$$P_{ExtBiloc}(a,b,c|x,y,z) = \int \rho_1(\lambda_1)\rho_2(\lambda_2)P(a|x,\lambda_1)P(b|y,\lambda_1,\lambda_2)P(c|z,\lambda_2)d\lambda_1 d\lambda_2 \tag{83}$$

which is exactly the form (78).

Conversely assume that P_{Biloc} is bilocal and therefore admits to the decomposition (78). Let $(\mu_1, \mu_2, \mu_3) = (x, y, z)$. This allows us to express $P(x)$ in a different form

$$P(x) = \int q_1(\mu_1)P(\mu_1)P(x|\mu_1)d\mu_1 \tag{84}$$

and similarly for $P(y)$ and $P(z)$. Since P_{Biloc} is bilocal we have

$$P_{Biloc}(a,b,c,x,y,z) = P_{Biloc}(a,b,c|x,y,z)P(x)P(y)P(z) \tag{85}$$

Performing (84) then yields the distribution given in (80).

■

Although this rather simple proof provides a way of avoiding the freedom of choice assumptions in star-networks, one must not draw the drastic conclusion that superdeterminism is now rejected from nature (although experimental result make it very likely) but simply emphasizes the fact that even if we assume superdeterminism, quantum mechanics still outperforms local realist correlations.

In order to realize an experiment not subject to the freedom-of-choice loophole, let the extended parties act as random number generators by distributing the uniformly mixed states $\frac{1}{2}(|0\rangle\langle 0| + |1\rangle\langle 1|)$ between edge parties and extended parties and allow extended parties to measure σ_z in order to obtain an outcome with uniform randomness.

The example we have provided for bilocality is straightforward to generalize to a broader statement. In fact given any star-network there always exists an extended star-network with fixed measurements such that the correlations in the star-network are n-local if and only if the correlations in the extended star-network are extended n-local. Once again, we interpret the outcomes of the extended parties as inputs of the edge parties.

4 Numerical case studies of quantum properties

Having provided Bell inequalities for four different star-network measurement scenarios and characterized the n-local set for qubit distribution we now study the quantum properties of the inequalities. We perform MatLab numerical analysis of case studies for star-networks with $n \geq 2$. We aim to provide violations of the inequalities with quantum probability distributions, find the maximal quantum violations, study properties of the quantumly attainable subset of the non n-local set.

Usually in foundational physics, the task we will consider in this section are often unmanageable to do directly by analytical tools. Unless one has an extraordinary intuition for quantum systems, one must be very lucky in order to solve the listed tasks analytically straight away. The common procedure is to first perform numerical studies to gain intuition in order to be able to show more general analytical results. Also, first performing the numerics will hopefully reduce the feeling of the rabbit being pulled out of the hat in section 5. Before we show the results of the numerical analysis we should say something about the numerical methods constructed for this section.

When increasing the number of parties the dimension of the composite hilbert space of the system increases exponentially. This implies that given arbitrary measurements for all parties involved in the system, computing the quantum probability distribution is a problem of exponential time computational complexity. This effectively puts a limit on how large networks we can analyze within reasonable time. Explicitly for the programs constructed for the tasks, the limits are n no larger than 4 for the $1 \rightarrow 2^n$ inequality and n no larger than 6 for the $2 \rightarrow 2$ inequality. A second problem arises from the fact that the n-local set is not convex i.e., that we have to perform nonlinear optimization over a more complicated set. Not only that the numerical methods for optimizing over non-convex sets are less efficient but also the fact that optimization algorithms can 'get stuck' in local extreme points is a problem. This fact makes the numerical analysis of the n-local assumption much more difficult than the Bell scenario where the local set is a convex polytope and the task of finding maximal violations is in comparison very easy. In some cases we try to overcome this problem by studying the n-local set along a linear path uniquely characterized by some number α, thus considering the optimal quantum violation along the linear path (OQVALPs).

Such a procedure allows for effective convex optimization since the straight line evidently is a convex subset of the n-local set and we can therefore use semi-definit programing (SDPs).

4.1 Examples of maximal quantum violations

Is it possible to find quantum probability distributions that violate the inequalities derived in section 3? To answer this question a suitable choice of states distributed between Bob and each of the n parties needs to be made. It is natural to consider one of the maximally entangled Bell states in equation (9). Let start with considering the $1 \to 2^n$ inequality and let each edge party in the bipartite star-network of n sources share the singlet Bell state with Bob

$$|\psi^-\rangle = \frac{1}{\sqrt{2}}\left(|01\rangle - |10\rangle\right) \tag{86}$$

We let Bob's measurement be a complete Bell state measurement on n qubits. Thus, the composite state of the n qubits at his disposal is projected onto a complete set of 2^n maximally entangled states. The essential and non-trivial question is which measurements the n parties should perform in order to maximize the quantities Q_1, Q_2 introduced in (54).

We now quantumly find these optimal measurements by brute force non-linear numerical optimization, starting with $n = 4$. The program fixes the complete Bell measurement of Bob and the states distributed between the parties while optimizing over the two possible measurements of each of the four edge parties which are in practice taken as linear combinations of the Pauli operators and identity since these span the space of 2×2 hermitian matrices. The maximal value returned by this numerical optimization for $n = 4$ is

$$\sum_{i=1}^{2} |Q_i|^{1/4} = 2^{1/4} \approx 1.19 \nleq 1 \tag{87}$$

This is a clear violation of the derived n-local bound, namely 1. Due to the nonlinear properties mentioned earlier it cannot be stated with 100 percent confidence that (87) constitutes the global maximal violation. Several other violations were observed constituting local maximums of the quantity being optimized. However after conducting extensive tests of the optimization by variation over the initial conditions it can be stated with confidence that (87) constitutes a maximal violation of the $1 \to 2^4$ inequality and it will be referred to as such. The maximal violation is obtained for

$$Q_1 = Q_2 = 0.125 \tag{88}$$

The measurements of the four parties corresponding to the obtained maximal violation of $1 \rightarrow 2^4$ inequality are symmetric linear combinations of the eigenvectors of σ_x and σ_y shifted by a relative phase to each other. We will not present the whole list of eigenvectors for reasons that will soon be obvious.

Having studied the case of $n = 4$ we now consider the case of $n = 3$. A similar brute force optimization was performed and a maximal violation of inequality $1 \rightarrow 2^3$ was obtained with high confidence. We now list all computed maximal violations of $1 \rightarrow 2^n$ inequality allowing us to spot a pattern.

$$n = 2: \qquad S^{1\rightarrow 2^n}_{max}(n = 2) = 2^{1/2} \approx 1.41 \nleq 1 \tag{89}$$
$$n = 3: \qquad S^{1\rightarrow 2^n}_{max}(n = 3) = 2^{1/3} \approx 1.26 \nleq 1 \tag{90}$$
$$n = 4: \qquad S^{1\rightarrow 2^n}_{max}(n = 4) = 2^{1/4} \approx 1.19 \nleq 1 \tag{91}$$

The factor by which quantum mechanics outperforms the n-local bound (the violation factor) seems to be exponentially decreasing with the number of edge parties and we therefore make the following conjecture.

Conjecture 1: The maximal quantum violation of the inequality $1 \rightarrow 2^n$ is given by $2^{1/n}$.

Due to this decreasing property, the $1 \rightarrow 2^n$ inequality is of less interest since we would like robustness also for large networks. We hope for better results with the $2 \rightarrow 2$ inequality.

When considereding the $2 \rightarrow 2$ inequality we choose a more effective approach than brute force optimization. We apply the previously described method of restricting ourselves to a line in the I, J-plane and use semi-definit programing to obtain the OQVALP. From the geometry of the n-local set and also from the results of maximal quantum violations for $1 \rightarrow 2^n$ it is a good guess to consider the path $I = J$ and find the corresponding OQVALP. In order to work with SDPs we fix the measurements of the edge parties to (σ_x, σ_z) and optimize over two POVMs for Bob, obeying

$$M_{b=0|y=0} + M_{b=1|y=0} = \mathbf{1} \qquad M_{b=0|y=1} + M_{b=1|y=1} = \mathbf{1} \tag{92}$$

Due to the constraint (92) we have the freedom of choosing a total of two POVMs for Bob.

Since the optimization is more effective than the previously applied brute force method we can generate OQVALPs for any $n \in \{2,3,4,5,6\}$:

$$S^{2\to 2}_{max}(2) = S^{2\to 2}_{max}(3) = S^{2\to 2}_{max}(4) = S^{2\to 2}_{max}(5) = S^{2\to 2}_{max}(6) = \sqrt{2} \nleq 1 \tag{93}$$

This is a remarkable result. In contrast to the $1 \to 2^n$ inequality, the maximal quantum violation does not decrease with n but seems to stay constant with the size of the network. However the POVMs of Bob realizing this maximal violation are not obvious nor reminiscent of any elementary measurement in quantum mechanics. Nevertheless they do uphold strong symmetries. This seems to suggest that there is a better choice of edge party measurements. In order to find these edge party measurements we first gain understanding of Bob's POVMs by realizing that they are on the form of the general parity operator. Introduce an arbitrary real qubit basis

$$B = \left\{ \begin{pmatrix} a \\ b \end{pmatrix}, \begin{pmatrix} -b \\ a \end{pmatrix} \right\} \qquad a^2 + b^2 = 1 \qquad a, b \in \mathbb{R} \tag{94}$$

By solving four systems of four linear equations one can find the parity observable corresponding to the basis B. For parity zero this is given by

$$\Pi^0_B = \frac{1}{(a^2+b^2)^2} \begin{pmatrix} a^4 + b^4 & a^3b - ab^3 & a^3b - ab^3 & 2a^2b^2 \\ a^3b - ab^3 & 2a^2b^2 & 2a^2b^2 & ab^3 - a^3b \\ a^3b - ab^3 & 2a^2b^2 & 2a^2b^2 & ab^3 - ba^3 \\ 2a^2b^2 & ab^3 - a^3b & ab^3 - a^3b & a^4 + b^4 \end{pmatrix} \tag{95}$$

Bob's measurement is of this form for $(a,b) = \left(\frac{\sqrt{2-\sqrt{2}}}{2}, \frac{\sqrt{2+\sqrt{2}}}{2} \right)$. This is an eigenvector of $\frac{\sigma_x + \sigma_z}{\sqrt{2}}$. Studying the parity one observable the second eigenvector is found. Similarly studying Bob's second measurement we find the eigenvectors of $\frac{\sigma_x - \sigma_z}{\sqrt{2}}$. Thus we can shift the basis of the complete star-system by letting the edge parties perform measurements

$$m_i = 0 : \qquad \frac{\sigma_x + \sigma_z}{\sqrt{2}} \tag{96}$$

$$m_i = 1 : \qquad \frac{\sigma_x - \sigma_z}{\sqrt{2}} \tag{97}$$

SDPs now give Bob's POVMs as parity measurements in the computational and diagonal bases respectively. For the special case of $n = 2$ these take the simple form corresponding to $a = b = \frac{1}{\sqrt{2}}$ and $a = 1, b = 0$ in (95) respectively.

$$M^{n=2}_{0|0} = \frac{1}{2}\begin{pmatrix}1 & 0 & 0 & 1\\ 0 & 1 & 1 & 0\\ 0 & 1 & 1 & 0\\ 1 & 0 & 0 & 1\end{pmatrix} \qquad M^{n=2}_{0|1} = \begin{pmatrix}1 & 0 & 0 & 0\\ 0 & 0 & 0 & 0\\ 0 & 0 & 0 & 0\\ 0 & 0 & 0 & 1\end{pmatrix} \tag{98}$$

Such a change of basis does not affect the maximal quantum violations in (93) but allows for better understanding of the quantum properties of the entanglement swapping measurement. In section 5 we will analytically prove that this sequence of measurement yields maximal quantum violations of $2 \to 2$ for a network of arbitrary size.

We continue with demonstrating that our bipartite qutrit inequality (52) is non-trivial. Consider the bilocality scenario and let the two sources distribute the maximally entangled state

$$|\psi\rangle = \frac{|00\rangle + |11\rangle + |22\rangle}{\sqrt{3}} \tag{99}$$

Inspired by the strong results of the $2 \to 2$ inequality we let Bob perform generalized parity measurements in the X and Z bases respectively. Then it is possible to obtain

$$\sqrt{|I_3|} + \sqrt{|J_3|} = \frac{4}{3} \nleq \frac{2}{\sqrt{3}} \tag{100}$$

The violation is rather small but it shows that it is a possible generalization to qutrits. Such an inequality will be interesting on its own but also in applications to detection efficiency for qubit distributions.

Finally we consider the multipartite inequality (69) and we pick the simplest non-trivial case depicted in figure 4 in section 3.5 with two three-partite sources. We have four quantities $K_\emptyset, K_{\{1\}}, K_{\{2\}}, K_{\{1,2\}}$ and we impose maximal freedom by allowing each quantity to be associated to one of four measurements for Bob. We choose to distribute GHZ-states in both sources

$$|GHZ\rangle = \frac{|000\rangle + |111\rangle}{\sqrt{2}} \tag{101}$$

and from the known properties of the GHZ-paradox we let all the edge parties perform the same measurements, namely σ_x and σ_y. Optimization over Bob's measurement yields a very strong maximal quantum violation of

$$S_Q^{2^{L-1}\to 2}(L=3,n=2)=2\nleq 1 \tag{102}$$

This result is obtained for Bob performing parity measurement in the bases given by the eigenvectors of σ_x and σ_y respectively. This demonstrates that one does not need the freedom of choosing four measurements for Bob, it is sufficient with two measurements ordered in such a way that all quantities K_X such that X is of even cardinality perform the same measurement and similarly for the odd cardinarlity quantities.

The violation factor of 2 is equivalent to the violation factor GHZ-states exhibit in the Mermin-inequality [37] with the same measurements and GHZ-states also uniquely maximally violate the Mermin inequalities [38]. Could it be the case that the nonlocality is in fact not arising from entanglement swapping but from the Bell scenario of each source i.e., between Alice, Albert and Bob in figure 4? Such suspisiouns are rejected by the fact that we can violate the inequality with a factor of $\sqrt{2}$ by letting Bob perform just one parity measurement in the diagonal basis so our scenario cannot be equivalent to the three-partite Bell scenario. Furthermore the robustness to increasing the number of sources also seems to hold true since we find

$$S_Q^{2^{L}\to 2}(L=3,n=3)=2\nleq 1 \tag{103}$$

For larger L, e.g. $L=4$ we see the same pattern. The $L=4$ bilocality inequality is maximally violated by Bob with such a configuration that for all quantities in (67) with X of even cardinality one measurement is associated and for all X of odd cardinality another measurement is associated. The zero-outcome measurement operator of these two measurements are

$$\frac{1}{2}\begin{pmatrix}1&0&0&-i\\0&1&1&0\\0&1&1&0\\i&0&0&1\end{pmatrix}\qquad\qquad\frac{1}{2}\begin{pmatrix}1&0&0&i\\0&1&1&0\\0&1&1&0\\-i&0&0&1\end{pmatrix} \tag{104}$$

by (92) the outcome-one operator is found for each of the two measurements in (104). The edge parties choose between measurements σ_x and σ_y. This configuration leads to the maximal violation

$$S_Q^{2^{4-1}\to 2}(L=4,n=2)=2\sqrt{2}\nleq 1 \tag{105}$$

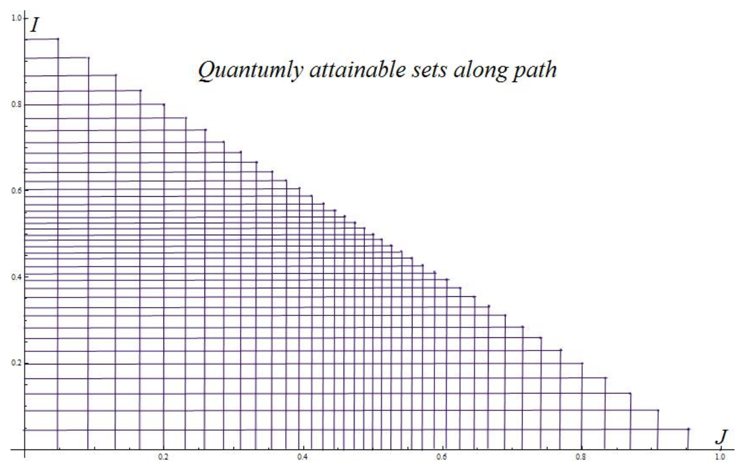

Figure 6: The set of quantumly attainable probability distributions for $n = 2$. Each rectangle represents the quantum set along the path.

It seems to be the case that we are reproducing violation factors that are equivalent to those of the Mermin inequality i.e., exponentially outperforming the local models and we make the following conjecture

Conjecture 2: The maximal quantum violation factor of inequality (69) describing the L-partite n-locality scenario is $2^{\frac{L-1}{2}}$. In section 5 we will introduce a general framework allowing the proof of this conjecture.

4.2 The set of quantum correlations

We have in section 3.4 we have studied the geometry of the n-local set of probability distributions. In this section we attempt the same task but for the quantum subset of the non n-local set attainable with inequality $2 \to 2$, restricting ourselves to $n = 2, 3$.

Introduce the path parameter α such that

$$I = \alpha J \tag{106}$$

defines a linear path in the I, J-plane on which we can apply SDPs. For $n = 2$ and $\alpha \in [0, 1]$ in steps of 0.05 we generate the OQVALPs corresponding to that particular value of α and $\frac{1}{\alpha}$ thus giving us 41 points on the boundary of the quantum subset of the non-bilocal set. Once finding the OQVALP for some α we numerically generate the set of quantum probability distributions

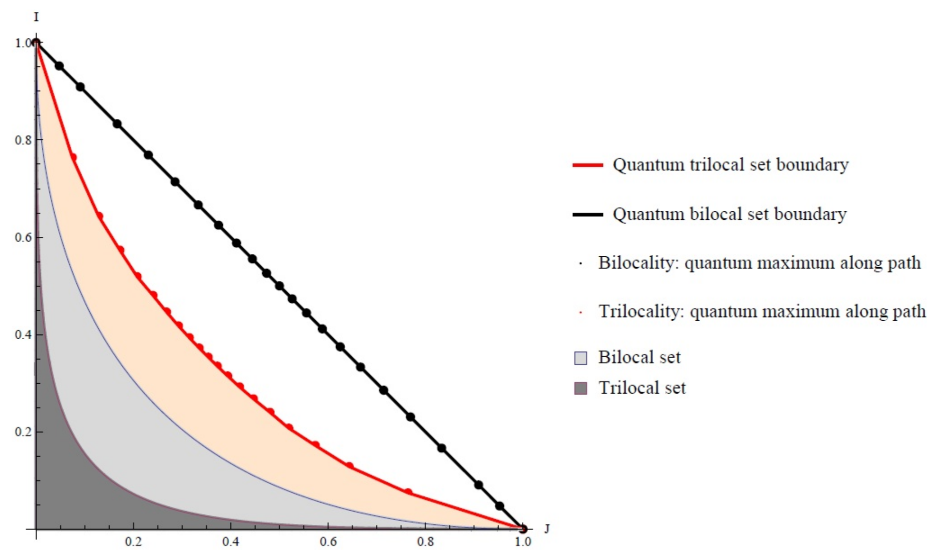

Figure 7: Bilocal and trilocal sets. Numerically obtained OQVALPs for $n = 2, 3$ are used to roughly draw the quantum subset of the non-bilocal and non-trilocal sets.

attainable along this path if the edge parties are allowed arbitrary measurements. We plot the result in figure 6. Each rectangle in the plot encloses the set of quantumly attainable probability distributions along the path. This rectangle formation derives from the fact that the only way the quantities I, J are coupled is through the measurements of the edge parties. Such a result would for instance not be expected for the $1 \to 2^n$ inequality.

Observe that the set boundary in figure 6 is linear and therefore equivalent to the local set arising in a Bell scenario (plotted also in figure 3). This raises interesting and fundamental questions about the nature of entanglement swapping versus shared randomness in terms of which correlations are attainable. Why should these two sets coincide?

In order to compare the quantum sets for different n we find, in a similar way to the $n = 2$ case, a set of OQVALPs for the $n = 3$ star-network. In figure 7 we display the data points on the boundaries of the quantum sets for $n = 2, 3$ together with an estimation of the set and the corresponding bilocal and trilocal sets.

The nonlinearity of the quantum set boundary arises in the trilocal case. Naturally the size of the quantum sets seem to be decreasing with n in

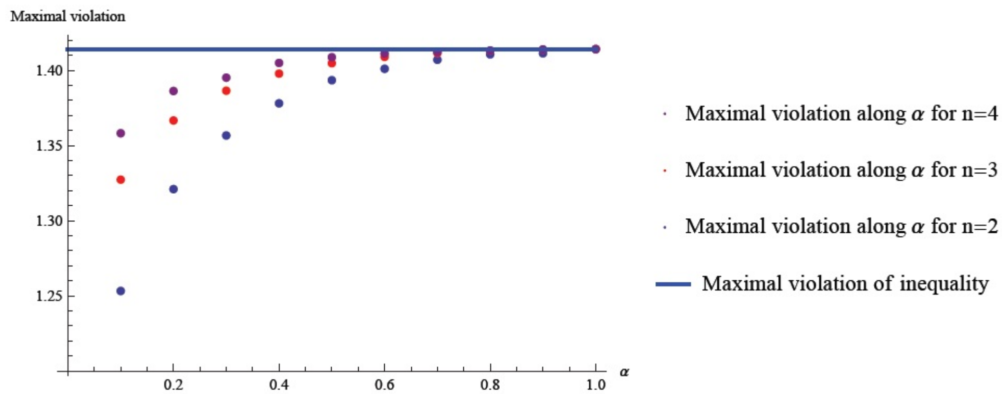

Figure 8: OQVALPs for $n = 2, 3, 4$.

analogy with the classical sets.

From section 4.1 we know that the maximal violations are all the same. However we have no information of how the violations behave along an arbitrary path in the I, J-plane for different values of n. We numerically study the violation factor of the inequality for $n = 2, 3, 4$ along paths $\alpha \in [0, 1]$ in steps of 0.1 and the results are shown in figure 8. Evidently the OQVALPs seem to be increasing with n. The sequence seems to be converging to the maximal violation of the inequality $\sqrt{2}$ quite rapidly. This suggests that the strength of the quantum correlations in the network for some given direction in the I, J-plane increases with the number of parties. The result make it plausible that in the limit when $n \to \infty$ the upper quantum bound

$$|I|^{1/n} + |J|^{1/n} \leq \sqrt{2} \tag{107}$$

will become a tight inequality for describing the quantumly attainable subset of the non n-local set.

5 Analytical studies of quantum properties

In the previous section we raised various questions about the quantum properties of the n-local set and the properties of OQVALPs which we treated with numerical analysis for small n. The central problem arose from the exponential growth of the probability distribution which in general constrains numerical studies. Nevertheless, in this section we will attempt an analytical approach to the questions raised in section 4 and show that the vast symmetries encountered in our n-locality inequalities allows for an effective analytical approach. We aim to provide a general analytical framework for analyzing quantum properties of our inequalities and use it to derive properties of quantum correlations both explaining and generalizing the numerical results of section 4.

5.1 Mathematical framework

We begin by introducing a general framework for analyzing our most general multipartite inequality (69). This will serve to demonstrate a general mathematical method rather than providing explicit computations which will be done in the next section.

Take the L-partite star-network measurement scenario with n sources that are all distributing GHZ-states. Let Bob choose from a set of arbitrary measurements and let each measurement be labeled y_X. Then the reduced state after Bob's measurements will in general be some mixture of pure states

$$\sum_j \mathscr{P}_j |\psi^j_{X,\Pi}\rangle\langle\psi^j_{X,\Pi}| \tag{108}$$

where Π is the outcome of the measurement y_X. Each edge party has two possible measurements that can be taken arbitrarily and we label the eigenvectors of these observables as $|m^k_j r^k_j\rangle$.

Introduce the following notations for the inner products

$$p^{j,k,l,X,\Pi}_{m^k_j, r^k_j} = \langle m^k_j, r^k_j|\psi^l_{X,\Pi}\rangle \tag{109}$$

Then the corresponding global probability distribution takes the form

$$P(\overline{r}|\overline{m}, y_X, \Pi) = \sum_l \mathscr{P}_l \left|\prod_{j,k} p^{j,k,l,X,\Pi}_{m^k_j, r^k_j}\right|^2 \tag{110}$$

In order to apply to our inequalities we just use that

$$P(\overline{r}, \Pi|\overline{m}, y_X) = P(\overline{r}|\overline{m}, y_X, \Pi)P(\Pi|y_X) \tag{111}$$

In principle, we can now compute the quantities K_X going into inequality (69), with more or less effort depending on the specification of measurements for all parties. However we know from the numerics which measurements for Bob are favorable.

In purpose of demonstration, let us fix the measurements of Bob to those found to yield maximal violations in section 4.1 leading to conjecture 2. For any odd L, applying the numerically obtained parity measurements and computing the reduced states will yield

$$\begin{aligned} |\kappa_1\rangle &\equiv \frac{1}{\sqrt{2}}\left(|0\rangle^{\otimes L-2} + (-1)^{y+\Pi}|1\rangle^{\otimes L-2}\right) \\ |\kappa_2\rangle &\equiv \frac{1}{\sqrt{2}}\left(|0\rangle^{\otimes \frac{L-2}{2}}|1\rangle^{\otimes \frac{L-2}{2}} + (-1)^{\Pi}|1\rangle^{\otimes \frac{L-2}{2}}|0\rangle^{\otimes \frac{L-2}{2}}\right) \\ \rho_{odd}^{y,\Pi} &= \frac{1}{2}|\kappa_1\rangle\langle\kappa_1| + \frac{1}{2}|\kappa_2\rangle\langle\kappa_2| \end{aligned} \tag{112}$$

Similarly for any even L the reduced state will be

$$\begin{aligned} |\mu_1\rangle &\equiv \frac{1}{\sqrt{2}}\left(|0\rangle^{\otimes L-2} - i(-1)^{y+\Pi}|1\rangle^{\otimes L-2}\right) \\ |\mu_2\rangle &\equiv \frac{1}{\sqrt{2}}\left(|0\rangle^{\otimes \frac{L-2}{2}}|1\rangle^{\otimes \frac{L-2}{2}} + (-1)^{\Pi}|1\rangle^{\otimes \frac{L-2}{2}}|0\rangle^{\otimes \frac{L-2}{2}}\right) \\ \rho_{even}^{y,\Pi} &= \frac{1}{2}|\mu_1\rangle\langle\mu_1| + \frac{1}{2}|\mu_2\rangle\langle\mu_2| \end{aligned} \tag{113}$$

When it comes to choosing edge party measurements it is known that the GHZ-states are trivial in the space spanned by σ_x and σ_z and without loss of generality we can consider only the xy-plane. Also assuming that all edge parties choose between the same measurements, we obtain

$$\begin{aligned} |m=0,r=0\rangle &= \frac{1}{\sqrt{2}}\begin{pmatrix}1\\ e^{i\theta}\end{pmatrix} \quad & |m=0,r=1\rangle &= \frac{1}{\sqrt{2}}\begin{pmatrix}1\\ -e^{i\theta}\end{pmatrix} \\ |m=1,r=0\rangle &= \frac{1}{\sqrt{2}}\begin{pmatrix}1\\ e^{i\phi}\end{pmatrix} \quad & |m=1,r=1\rangle &= \frac{1}{\sqrt{2}}\begin{pmatrix}1\\ -e^{i\phi}\end{pmatrix} \end{aligned} \tag{114}$$

for some ϕ, θ. Having computed reduced states and defined the edge party measurement eigenvectors it is straightforward to compute $p^{j,k,l,X,\Pi}_{m^k_j,r^k_j}$ from which the all K_X can be found. Observe that chosing $\theta = 0$ and $\phi = \frac{\pi}{2}$ will return the measurement scenario seen to produce maximal violations in section 4.1. In the next section we show an explicit example of this method.

5.2 Sequence of maximal quantum violations

The framework of the previous section will here be used to solving the problem of providing a sequence of measurements that will maximally violate the inequality $2 \to 2$ for any n i.e., show that the numerical results in (93) indeed are true for arbitrary large networks. We do this by studying the state of the system after Bob's measurement and show that this is an entangling measurement leading to strong symmetries. On basis of our numerics favoring parity measurements for Bob we derive a lemma.

Lemma 2:(State post Bob). Given a bipartite star-network configuration with $d = 2$ of n shared singlet states and Bob performing one of two possible measurements $\{\Pi_{comp}, \Pi_{diag}\}$ labeled by $y = 0, 1$ corresponding to parity in computational and diagonal basis respectively, the reduced state of the system is

$$|\psi^{\Pi}_{y=0}\rangle = \frac{1}{\sqrt{2}}\left(|+\rangle^{\otimes n} + (-1)^{\Pi}|-\rangle^{\otimes n}\right) \tag{115}$$

$$|\psi^{\Pi}_{y=1}\rangle = \frac{1}{\sqrt{2}}\left(|0\rangle^{\otimes n} + (-1)^{\Pi}|1\rangle^{\otimes n}\right) \tag{116}$$

Proof:

Distributing n copies of the singlet state yields the global state of the system to be

$$|\psi\rangle = \bigotimes_{i=1}^{n} |\psi^-\rangle \tag{117}$$

Temporarily introduce the notation $p = |01\rangle$ (p-block) and $q = |10\rangle$ (q-block). Define some operation such that $N(p) = 0$ and $N(q) = 1$ and expand (117) in a sum 2^n unique terms consisting of n blocks with some combination of blocks of type p, q.

$$|\psi\rangle = \sum (-1)^{N(q)} perm\{p, q\}^{\otimes n} \tag{118}$$

It is important to keep the ordering of the hilbert spaces in mind.

Introduce Bob's first measurement, $y = 0$ i.e., parity in computational basis. Assume that the outcome is $\Pi = 0$. If the number of $|1\rangle$ vectors in the tensor product on Bob's hilbert spaces is even then, these will be projected onto them selves with eigenvalue 1. Otherwise the parity-zero measurement operator associates the eigenvalue to 0.

The number of vectors on $\mathscr{H}_{Bob}$ with parity zero is given by the number of ways one can positition an even number of $|1\rangle$-vectors in the tensor product of Bob i.e.,

$$\sum_{i=0}^{n} \binom{n}{2i} = 2^{n-1} \tag{119}$$

The same will of course hold for the outcome $\Pi = 1$ of measurement $y = 0$.

Thus the reduced state of the system after Bob perform his measurement is

$$|\psi_{y=0}^{\Pi=0}\rangle = \frac{1}{\sqrt{2^{n-1}}} \sum_{x_1 \oplus ... \oplus x_n = 0} |x_1 x_2 ... x_n\rangle \tag{120}$$

$$|\psi_{y=0}^{\Pi=1}\rangle = -\frac{1}{\sqrt{2^{n-1}}} \sum_{x_1 \oplus ... \oplus x_n = 1} |x_1 x_2 ... x_n\rangle \tag{121}$$

We now show that the reduced states (120,121) in fact are maximally entangled states. This would imply that the measurements of Bob are entangling measurements, swapping the entanglement of the global system. We apply the method of induction.

Define the diagonal ON-basis of qubit state space as

$$|+\rangle = \frac{1}{\sqrt{2}}\left(|0\rangle + |1\rangle\right) \qquad |-\rangle = \frac{1}{\sqrt{2}}\left(|0\rangle - |1\rangle\right) \tag{122}$$

Then it is straightforward to show that the following two Bell states are subject to rotational symmetry with respect to the diagonal basis

$$|\phi^+\rangle \equiv \frac{1}{\sqrt{2}}\left(|00\rangle + |11\rangle\right) = \frac{1}{\sqrt{2}}\left(|{+}{+}\rangle + |{-}{-}\rangle\right) \tag{123}$$
$$|\psi^+\rangle \equiv \frac{1}{\sqrt{2}}\left(|01\rangle + |10\rangle\right) = \frac{1}{\sqrt{2}}\left(|{+}{+}\rangle - |{-}{-}\rangle\right)$$

Holding true for $n = 2$, this constitutes the base case for our induction assumption that given any $n > 2$

$$|\psi_{y=0}^{\Pi=0}\rangle = \frac{1}{\sqrt{2^{n-1}}} \sum_{x_1 \oplus ... \oplus x_n = 0} |x_1 x_2 ... x_n\rangle = \frac{1}{\sqrt{2}}\left(|+\rangle^{\otimes n} + |-\rangle^{\otimes n}\right) \tag{124}$$

$$|\psi_{y=0}^{\Pi=1}\rangle = \frac{1}{\sqrt{2^{n-1}}} \sum_{x_1 \oplus ... \oplus x_n = 1} |x_1 x_2 ... x_n\rangle = \frac{1}{\sqrt{2}}\left(|+\rangle^{\otimes n} - |-\rangle^{\otimes n}\right) \tag{125}$$

We perform the induction for (124). Take $k = n + 1$ and use the induction assumption together with (122) to obtain

$$\begin{aligned}
\frac{1}{\sqrt{2^{k-1}}} \sum_{x_1 \oplus \ldots \oplus x_k = 0} |x_1 x_2 \ldots x_k\rangle = |0\rangle \otimes \frac{1}{\sqrt{2^{k-1}}} \sum_{x_2 \oplus \ldots \oplus x_k = 0} |x_2 \ldots x_k\rangle + \\
|1\rangle \otimes \frac{1}{\sqrt{2^{k-1}}} \sum_{x_2 \oplus \ldots \oplus x_k = 1} |x_2 \ldots x_k\rangle = \\
|0\rangle \otimes \frac{1}{\sqrt{2}} \left(|+\rangle^{\otimes k-1} + |-\rangle^{\otimes k-1} \right) + |1\rangle \otimes \frac{1}{\sqrt{2}} \left(|+\rangle^{\otimes k-1} - |-\rangle^{\otimes k-1} \right) = \\
(|0\rangle + |1\rangle) \otimes |+\rangle^{\otimes k-1} + (|0\rangle - |1\rangle) \otimes |-\rangle^{\otimes k-1} = \frac{1}{\sqrt{2}} \left(|+\rangle^{\otimes k} + |-\rangle^{\otimes k} \right) \quad (126)
\end{aligned}$$

An analog argument will prove (125).

Due to the rotational symmetry of the singlet state, one can almost copy this proof to show that the relation (116) hold true for Bob's second measurement, Π_{diag}.

∎

Having the lemma in place we demonstrate a sequence of maximal violations of the $2 \to 2$ inequality.

Theorem 6: (Maximal quantum violation) Given a bipartite star-network configuration with $M = d = 2$ of n shared singlet states a sequence of measurements yielding a violation of inequality (30) by a factor of $\sqrt{2}$ is letting the edge parties all make the measurements in (96,97) and let Bob perform parity measurements in the computational and diagonal bases respectively: $\{\Pi_{comp}, \Pi_{diag}\}$.

Proof:

The parties on the edges perform their measurements provided in (96,97). Label the sequence of measurements by $\overline{m}$ and the sequence of outcomes by $\overline{r}$. We know that the reduced states tracing out Bob's hilbert space are maximally entangled pure states. As a special case of our general framework, applying lemma 2 together with (110,111) we can compactly present the probability distributions given the measurement of Bob.

$$P(\overline{r}, \Pi | \overline{m}, y = 0) = \frac{1}{4}\Big| \prod_{i=1}^{n} \langle m_i, r_i | + \rangle + (-1)^{\Pi} \prod_{i=1}^{n} \langle m_i, r_i | - \rangle \Big|^2 \tag{127}$$

$$P(\overline{r}, \Pi | \overline{m}, y = 1) = \frac{1}{4}\Big| \prod_{i=1}^{n} \langle m_i, r_i | 0 \rangle + (-1)^{\Pi} \prod_{i=1}^{n} \langle m_i, r_i | 1 \rangle \Big|^2 \tag{128}$$

Observe that the probability distribution exhibits strong symmetries in the sense that it does not matter which party is doing what measurement and obtaines which outcome. We are only concerned about the number of people making some measurement and obtaining some outcome. This motivates some new notations. Let α be the number of parties making measurement zero obtaining outcome zero, β the number of parties making measurement zero obtaining outcome one, γ the number of parties making measurement one obtaining outcome zero and δ the number of parties making measurement one obtaining outcome one. Evidently it must hold true that $\alpha+\beta+\gamma+\delta = n$.

Since we can completely map each probability distribution by essentially computing eight inner products, the task is very simple. Calculating the eigenvectors of the edge party measurements and taking the respective inner products with $|+\rangle$ and $|-\rangle$ we can reduce (127) to

$$\begin{aligned} P_{y=0}(\alpha, \beta, \gamma, \delta, \Pi) = \frac{1}{2^{1+2n}} \big| &(2-\sqrt{2})^{\frac{\alpha+\delta}{2}} (2+\sqrt{2})^{\frac{\beta+\gamma}{2}} + \\ &(-1)^{\alpha+\gamma+\Pi} (2-\sqrt{2})^{\frac{\beta+\gamma}{2}} (2+\sqrt{2})^{\frac{\alpha+\delta}{2}} \big|^2 \end{aligned} \tag{129}$$

where $\Pi \in \{0, 1\}$ is outcome of Bob's parity measurement. The similar computation for (128) is simple.

The quantity I can now explicitly be decomposed in terms of the distribution (129). One has to account for the degeneracy of the measurement settings and outcomes by introducing multinomial coefficients. Similar procedure for (128) yields

$$
\begin{aligned}
I \equiv \frac{1}{2^n} \sum_{\overline{m},\overline{r},b} (-1)^{r_1+\ldots+r_n+b} P(\overline{r}, b|\overline{m}, y=0) = \\
= \frac{1}{2^n} \sum_{\Pi=0,1} \sum_{\alpha+\beta+\gamma+\delta=n} (-1)^{\beta+\delta+\Pi} \binom{n}{\alpha,\beta,\gamma,\delta} P_{y=0}(\alpha,\beta,\gamma,\delta,\Pi) \\
J \equiv \frac{1}{2^n} \sum_{\overline{m},\overline{r},b} (-1)^{r_1+\ldots+r_n+b} P(\overline{r}, b|\overline{m}, y=1) = \\
= \frac{1}{2^n} \sum_{\Pi=0,1} \sum_{\alpha+\beta+\gamma+\delta=n} (-1)^{\beta+\gamma+\Pi} \binom{n}{\alpha,\beta,\gamma,\delta} P_{y=1}(\alpha,\beta,\gamma,\delta,\Pi)
\end{aligned}
\tag{130}
$$

The domain of the summation over $\alpha, \beta, \gamma, \delta$ can equivalently be expressed as all possible partitions of n into four non-negative integers.

Finding I, J for the introduced measurements for the edge parties is now a matter of direct calculation. Some simplification will yield the probability distribution on the form

$$
P_{y=0} = \frac{1}{2}\left(\frac{2+\sqrt{2}}{4}\right)^n \left(\left(\frac{2-\sqrt{2}}{2+\sqrt{2}}\right)^{\alpha+\delta} + \left(\frac{2-\sqrt{2}}{2+\sqrt{2}}\right)^{n-\alpha-\delta} + 2(-1)^{\alpha+\gamma+\Pi}\left(\sqrt{2}-1\right)^n \right) \tag{131}
$$

We can immediately realize that the first two terms in the brackets do not contribute to I, J since they are symmetric in Π. Only the third term in (131) contributes and some simplification will give the final result

$$
I = (-1)^n \left(\frac{1}{4\sqrt{2}}\right)^n \sum_{\alpha+\beta+\gamma+\delta=n} \binom{n}{\alpha,\beta,\gamma,\delta} = \frac{(-1)^n}{\sqrt{2^n}} \tag{132}
$$

An analog analysis for J will give

$$
|J| = \frac{1}{\sqrt{2^n}} \tag{133}
$$

The implication for inequality (30) is

$$
|I|^{1/n} + |J|^{1/n} = \sqrt{2} \tag{134}
$$

$\blacksquare$

The method introduced in this proof also provides extensive numerical computational power for n-locality problems in general. In previous evaluation of the inequalities (30) and (55) we have applied nonlinear optimization programs of high computational complexity resulting in the inability of analyzing large networks. Even with the SDPs we could not go beyond $n = 6$ in any realistic time. However by keeping the parity measurement of Bob and varying the measurements of the edge parties the distributions (127,128) can easily be modified for various inner products. Each correlator, first introduced in (27) as a linear combination of probabilities can then with few steps be computed from the distribution function.

In addition, one should observe the following: The fact that we can make such a manageable analysis of a network of arbitrary size is fully due to the nature of the entanglement swapping performed by the parity measurement i.e., the simple structure of the reduced state after Bob's measurement in lemma 2.

5.3 Parity generated quantum non n-local sets

We now further explore the quantum non n-local set as generated through Bob's parity measurements. Even though our previous method allows for very efficient numerical computations, we can analytically explore its generalized forms. In this section we show how the post Bob's measurement symmetries allows for a complete characterization the quantum n-local set generated with parity measurements by Bob.

Fix Bob's measurements to parity in computational and diagonal bases so that the post-measurement symmetries arise according to lemma 2. For edge party measurements we parametrize these to a general form as follows

$$\left\{\begin{pmatrix}-\sin\left(\frac{\phi}{2}\right)\\ \cos\left(\frac{\phi}{2}\right)\end{pmatrix},\begin{pmatrix}\cos\left(\frac{\phi}{2}\right)\\ \sin\left(\frac{\phi}{2}\right)\end{pmatrix}\right\}\qquad\left\{\begin{pmatrix}-\sin\left(\frac{\theta}{2}\right)\\ \cos\left(\frac{\theta}{2}\right)\end{pmatrix},\begin{pmatrix}\cos\left(\frac{\theta}{2}\right)\\ \sin\left(\frac{\theta}{2}\right)\end{pmatrix}\right\} \tag{135}$$

The parameters (ϕ, θ) are by (135) associated to the two eigenvectors of the qubit measurement. Applying the analytical introduced in the previous sections, we can after some computations show that

$$I(\theta,\phi) = \frac{1}{4^n} \sum_{\alpha+\beta+\gamma+\delta=n} \binom{n}{\alpha,\beta,\gamma,\delta} (-1)^{n+\delta+\gamma} \cos^{\alpha+\beta}(\phi) \cos^{\gamma+\delta}(\theta) \quad (136)$$

$$J(\theta,\phi) = \frac{1}{4^n} \sum_{\alpha+\beta+\gamma+\delta=n} \binom{n}{\alpha,\beta,\gamma,\delta} (-1)^{\delta+\gamma} \sin^{\alpha+\beta}(\phi) \sin^{\gamma+\delta}(\theta) \quad (137)$$

The multinomial theorem allows us to write (136,137) in a much more compact form

$$I(\theta,\phi) = \frac{(-1)^n}{2^n} \left(\cos(\phi) - \cos(\theta)\right)^n \qquad J(\theta,\phi) = \frac{1}{2^n} \left(\sin(\phi) - \sin(\theta)\right)^n \quad (138)$$

At this point we can see that the case of maximal quantum violations obtained in theorem 6 is the special case of (138) corresponding to $\theta = \frac{5\pi}{4}$ and $\phi = \frac{\pi}{4}$.

Due to the form of inequality (30) it is evident that the value of the inequality corresponding to $I(\theta,\phi), J(\theta,\phi)$ is independent of n. We write it as

$$S_Q^{2\to 2} = \frac{1}{2} \left(|\cos(\phi) - \cos(\theta)| + |\sin(\phi) - \sin(\theta)|\right) \quad (139)$$

Given any ϕ i.e., fixing one edge party measurement, there is a subset of the quantum non n-local set that is realizable with the freedom of varying θ. Since ϕ is a continuous parameter there are infinitely many such cases and the union of these enclosed sets corresponds to the quantum non n-local set in the I, J-plane generated through parity measurements. Furthermore, given any ϕ there exists a θ such that the corresponding probability distribution corresponds to a OQVALP for some specified path parameter α. We parametrically plot the values of $I(\theta), J(\theta)$ for different values of ϕ for the special cases of $n = 2, 3$ to demonstrate the power of this method for identifying quantum sets. See figures 9 and 10.

From our numerical studies in section 4 we have sufficient data on the quantum set boundaries in order to compare with the analytical results. For the case of $n = 2$ we compare to the local set boundary since (as pointed out in section 4) the quantum non bilocal set and the local set are the same. For $n = 3$ we use the numerically obtained boundary function.

Now we are ready to solve the final problem. Completely characterizing the quantum non n-local set induced by parity measurement. The importance of this lies in the following fact we will be able to determine if some

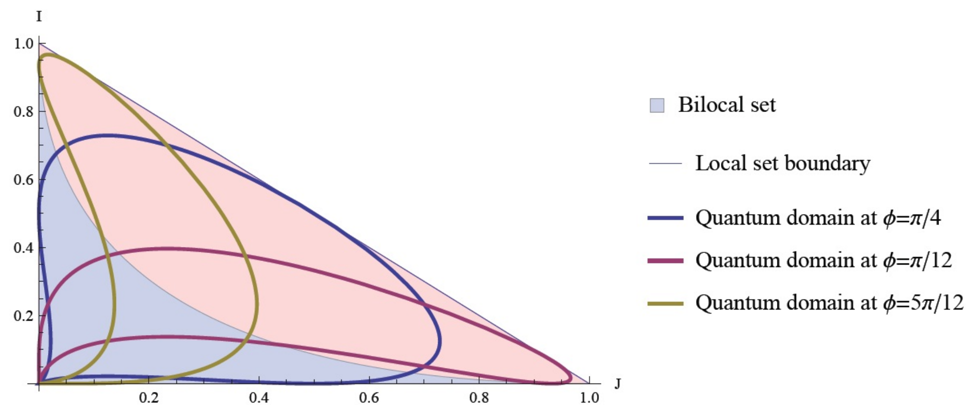

Figure 9: Quantumly attainable sets in the I, J-plane for various ϕ for $n = 2$. The sets are compared to the bilocal set and the in section 4 numerically obtained quantum sets to demonstrate a sequential mapping of the quantum non-bilocal set.

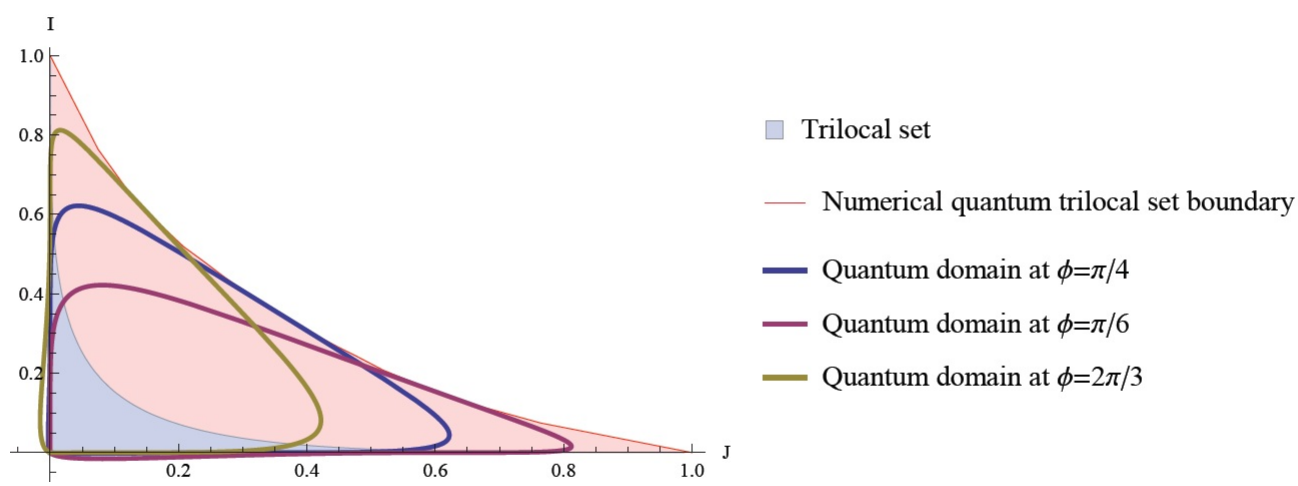

Figure 10: Quantumly attainable sets in the I, J-plane for various ϕ for $n = 3$. The sets are compared to the trilocal set and the in section 4 numerically obtained quantum set to demonstrate a sequential mapping of the quantum non-trilocal set.

probability distribution is detected by the inequality as supra quantum. Evidently the quantum upper bound of $\sqrt{2}$ is in no way tight which we saw in section 4. However we can now give a proper characterization of the quantum set solving this problem. We do this by realizing that the set of points (I, J) corresponding to OQVALPs generated by variation of ϕ and optimization over θ is the upper quantum set bound.

The set of OQVALPs is easy to recover. From (138) it is obvious that for $\phi = \theta$ the inequality is zero. A shift by π between the angles such that $\phi = \theta - \pi$ then generates the optimum. For these optimal choices of measurements (138) simplifies to

$$I(\theta) = (-1)^n \cos^n(\theta) \qquad J(\theta) = \sin^n(\theta) \tag{140}$$

Thus we have fully characterized the quantum n-local set generated through partiy measurements. Testing these against the numerically obtained bounds in section 4 indeed yields very good agreement.

As a corollary of (138) we can now solve the problem of finding measurements generating the corresponding OQVALP for given path. Along the path associated to α i.e., $I = \alpha J$ we can now easily obtain the following relation

$$\theta = \operatorname{arccot}\left(\alpha^{1/n}\right) \tag{141}$$

Let us make some observations on basis of equation (140). Some rather interesting phenomena is exhibited by the quantum sets in comparison to the n-local sets. Given any non-negative n we can rewrite I, J such that

$$I = \left(\cos^2(\theta)\right)^{n/2} \qquad J = \left(1 - \cos^2(\theta)\right)^{n/2} \tag{142}$$

which is subject to the relation

$$|I|^{2/n} + |J|^{2/n} = 1 \tag{143}$$

Assuming that n is an even integer (so that we have a physical interpretation), expression (143) exactly corresponds to the $\frac{n}{2}$-local set as described by inequality (30). However since the quantities I, J are not the same for different n we cannot conclude some equivalence between n-local set and the quantum non $2n$-local set. However this property is remarkable and surely leads to several new questions on the nature of quantum correlations in entanglement swapping configurations.

6 Experimental imperfections and quantum correlations

In this section we are concerned with the possibility of observing quantum correlations in a star-network under realistic experimental conditions. For any such real-life task experimental imperfections cause the effectively observable value of Bell inequalities to decrease. Depending on the intensity of these experimental imperfections, quantum correlations may be impossible to observe thus rendering applications useless.

The two most significant imperfections arise from 1) detectors not having ideal detection rates. Depending on the type of experiment the efficiency of detectors can vary a lot. If one is performing experiment on entangled photons one can roughly speaking expect lower detection efficiencies than e.g. experiments one entangled ions.[5] 2) Random signals causing disturbances known as noise. Noise can come of many forms (different colors) but the most relevant one is white noise where the random disturbances have constant power spectral density i.e., flat distributions. We study how much experimental imperfections our inequalities can be subject to and still uphold quantum correlations.

6.1 Only one ideal detector

The first case we consider is the star-network of n edge parties where central party Bob has a perfect detector while the edge party detectors are all subject to inefficiencies. Since all edge parties perform one-qubit measurements it is realistic to assume that they are all subject to the same inefficiency $\eta \in [0, 1]$ defined as the probability that a qubit is successfully detected. Thus $\eta = 1$ is the same as a perfect detector.

Every time a party fails to detect a qubit the party outputs some number, for simplicity 0 but can in general be chosen with any deterministic strategy. We then numerically compute the critical detection efficiency $\eta_{critical}$ at which it is no longer possible to observe quantum correlations. For the case of inequality (30) at the most elementary case of $n = 2$ we find

$$\eta_{critical}^{n=2} = \frac{1}{\sqrt{2}} \tag{144}$$

[5] On the other hand spin entangled ions are subject to other shortcomings such as the locality loophole.

This strong result is already known from [30]. We expect it to hold for any n due to theorem 6 and the fact that Bob has a perfect detector so the increased complexity of the parity measurement is not taken into account.

For inequality (55) where Bob is performing complete Bell state measurement we have studied the inefficiencies for $n = 2, 3, 4$ and we find

$$\begin{aligned} \eta_{critical}^{n=2} &= 2^{-1/2} \approx 0.71 \\ \eta_{critical}^{n=3} &= 2^{-1/3} \approx 0.79 \\ \eta_{critical}^{n=4} &= 2^{-1/4} \approx 0.84 \end{aligned} \tag{145}$$

The exponential decrease in the optimal quantum violations observed in section 4.1 seems to be inversely related to the critical detection efficiency. This result clearly implies that large scale star-networks will run into experimental problems.

There should be no doubt that the scenario we are considering is unfair. The low critical detection efficiencies we have obtained cannot fairly be compared to the CHSH-inequality where the critical detection efficiency is 82.8% [39] with inefficiency on both detectors involved. We cannot argue that we have objectively lowered the requirements of observing quantum correlations. However it is interesting to observe that for $n = 3$ and with complete Bell measurement we are encountering a scenario where we have one perfect detector and three inefficient detectors and that the corresponding critical detection efficiency is actually lower than for the two detectors in CHSH. Equation (145) shows us that this property is lost already for $n = 4$, however it will always be true for inequality (30).

6.2 All detectors inefficient

The issue with properly quantifying detection ineffi""cy in star-networks comes from Bob's measurement. With increasing n the complexity of this measurement significantly increases. For inequality (55) the problems are too great for us to propose a satisfying solution since the complete Bell measurement even in theory is impossible to perform with linear optics and would require a number of detectors exponentially growing with n.

On the other hand we have seen that inequality (30) can be realized with linear optics. Parity measurement is of significantly smaller complexity than complete Bell measurements. Nevertheless, the problem of how to quantify the n-qubit measurement is not obvious and one may want to consider several

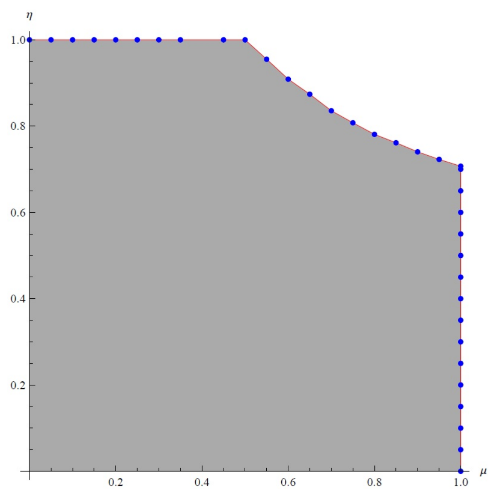

Figure 11: The region in the $\eta\mu$-plane where quantum correlations cannot be observed by inequality (30) for the bilocal case. The blue dots are the numerical datapoints.

quantifications each corresponding to some interpretation of the experimental procedure of measuring parity. We now present one such quantification and thus considering a scenario where all detectors are subject to inefficiencies.

There is no reason for the inefficiency of Bob to be the same as the edge parties. Let the detection efficiency of the edge parties be η and the efficiency of Bob to be μ. In this model, Bob's efficiency is linear however in some experimental realizations it has to be taken quadratic. We now consider the case of $n = 2$ for inequality (30). Keeping $\eta = 1$ it is observed that the inequality is fairly robust against Bob's measurement failing. The efficiency can then be taken as low as $\mu = \frac{1}{2}$. In figure 11 we roughly display the region in the $\eta\mu$-plane where it is not possible to violate the inequality on basis of the data points on the boundary obtained by numerical analysis (blue dots).

There is no natural way of telling whether we have lowered the requirements of observing quantum correlations in comparison to CHSH or not due to the distinct nature of the two measurement scenarios. A proposition for measuring this would be to consider the supremum of the set of geometric means of the efficiencies of all detectors involved along the nontrivial part of the critical boundary. In terms of this measure, we would outperform the 82.8% obtained in CHSH.

Another possible measure is to restrict ourselves to the line $\eta = \mu$ and then simply take the inefficiency of each detector as a measure of the critical efficiency of the overall system. Such a procedure leads to

$$\eta_{critical} \approx 0.791 \pm 0.005 \tag{146}$$

which is lower than the CHSH critical efficiency.

As a final remark: there are various ways to quantify detection efficiencies. In the model applied here we say that if a qubit is not detected by some party, this party always outputs a 0. There is a method of higher potential relying on quantifying the failed detections as an outcome on its own. Thus the measurements of the edge parties would be regarded as three-outcome measurements. However this is not compatible with the form of the inequalities (30,55) but is more intimately connected with generalizing n-local inequalities to arbitrary dimensions. The inequality (52) could be used for this purpose. However it may be the case that a stronger inequality will be necessary. This approach to detection efficiency is left as an open question.

6.3 Resistance to white-noise

The resistance to white noise is an important property that needs to be studied in terms of how much noise a quantum probability distribution can be subject to and still violate the $1 \to 2^n$ inequality. This task we solve analytically for the inequality (55) but it is straightforward to realize that with slight modification the argument also holds for all our derived inequalities due to the linearity in the correlation functions.

Assume that each of the n sources S_i instead of sending the maximally entangled state send white noise with a probability $1 - v_i$. Thus the state actually transmitted by source S_i is not a pure state but the mixed state described by the density matrix

$$\rho_i(v_i) = v_i|\phi_{00}\rangle\langle\phi_{00}| + (1 - v_i)\,\frac{\mathbf{1}}{2^n} \tag{147}$$

The white noise is represented by a flat distribution i.e. the identity operator. Thus the total visibility of the n-party system is $V = v_1 v_2 \dots v_n$. The states of highest interest are those presented in section 4.1 maximally violating the inequalities. The quantum probability distribution P_Q is subject to white noise and takes a dependence on V.

$$P_Q(V) = VP_Q + (1-V)P_0 \tag{148}$$

where $P_0 = P_0(r_1,\dots,r_n,b^1b^2\dots b^n|m_1,m_2,\dots,m_n) = \left(\frac{1}{2^n}\right)^2; \forall r_i, b^i, m_i;$ is the uniform probability distribution. Recalling the definition of the introduced correlator in (53) implemented with $P_Q(V)$:

$$\langle B^y C^1_{m_1}...C^n_{m_n}\rangle_V = \sum_{b^1...b^n,r_1,...,r_n} (-1)^{b^y+\sum_{i=1}^n r_i} P_Q(V)(b^1...b^n,r_1,...,r_n|m_1,...,m_n) \tag{149}$$

As seen in (148) there are two terms going into $P_Q(V)$ however the second of these will not contribute to the correlator since P_0 is a constant and as all the variables of the sum are binary the terms can be grouped in pairs of opposite signs and cancel out. The correlator (150) simplifies to

$$\langle B^y C^1_{m_1}...C^n_{m_n}\rangle_V = \sum_{b^1...b^n,r_1,...,r_n} (-1)^{b^y+\sum_{i=1}^n r_i} VP_Q(b^1...b^n,r_1,...,r_n|m_1,...,m_n) \tag{150}$$

Thus the visibility can be factored out the quantities Q_i may therefore be written

$$Q_i(V) = VQ_i \tag{151}$$

Thus inequality (55) taking white noise into account becomes

$$|Q_1(V)|^{1/n} + |Q_1(V)|^{1/n} = V^{1/n}\left(|Q_1|^{1/n} + |Q_1|^{1/n}\right) \leq 1 \tag{152}$$

If we denote $S_{max}(n)$ the maximal violation of inequality (55) for a given n then we have the critical visibility

$$V_{critical} = \prod_{i=1}^n v_i = \left(\frac{1}{S_{max}(n)}\right)^n \tag{153}$$

for which it is no longer possible to observe quantum correlations in the star-network.

A realistic assumption is that the n sources available are subject to the same visibilities i.e. $v = v_i \quad \forall i \in \mathbb{N}_n$ thus implying the total visibility $V = v^n$ and yielding the critical visibility of each source

$$v_{critical} = \frac{1}{S_{max}(n)} \tag{154}$$

Considering $1 \to 2^n$ inequality the critical bound is best for $n = 2$ yielding $v_{critical} = \frac{1}{\sqrt{2}}$ and then decreasing exponentially with n. However considering the $2 \to 2$ inequality the critical visibility stays constant at $v_{critical} = \frac{1}{\sqrt{2}}$ for any n. This means that arbitrarily large networks can be constructed with non-increasing critical visibility. The implication for the multipartite inequality (69) is that we have an exponentially decreasing critical visibility

$$v_{critical} = \frac{1}{\sqrt{2^{L-1}}} \tag{155}$$

which is equivalent to the critical visibilities for the Mermin inequality.

A concluding remark: One might observe that choosing to count detection inefficiencies by letting a failed measurement randomly be associated to 0 or 1 is in fact equivalent to our treatment of white noise and therefore the argument of this section shines some light on this special interpretation of inefficient detection.

7 Conclusions

In this thesis we have examined entanglement swapping in a broad class of star-networks. We characterized local realist theories for such networks by introducing the n-local assumption and from it we derived four Bell inequalities: two inequalities involving qubit distribution with n bipartite sources, one inequality involving qutrit distribution by the sources and one inequality generalizing the concept to multipartite sharing of hidden variables.

For the case of bipartite qubit distribution we found a family of LHVs used to prove tightness of our inequalities with respect to the n-local set and it is left as an open question to prove or disprove the tightness property for the multipartite inequality (69).

Having derived Bell inequalities we continued with numerical studies of the inequalities and presented a range of examples of maximal violations for the inequalities. This lead us to the conclusion that the optimal quantum violations were decreasing for inequality (55) while remaining constant for inequality (30) and exponentially increasing for inequality (69). We continued by numerical studies of various properties of the quantum sets for $n = 2, 3$ for inequality (30). We demonstrated equivalence between the quantum nonbilocal set and the local polytope but maintain that the nonlinearity of the

n-local assumption cause the quantum sets to have non-convex rather complicated boundaries. Why the quantum non-bilocal set and the local polytope coincide is an open question.

By observing basic symmetries of the Bob's measurement we gave proof of measurement settings yielding maximal violations of (30) for any n. Essentially our introduced method strongly reduces the computational complexity of analyzing the quantum properties in problems involving entanglement swapping in star-networks. Furthermore we analytically derived the full characterization of the quantum non n-local sets induced by parity measurements showing unexpectedly simple structures.

We also studied the behavior of quantum correlations in presence of experimental imperfections. We studied inequality (30) and (55) in an unfair scenario with inefficient detectors. Even though we show a critical detection of $\frac{1}{\sqrt{2}}$ for $n = 2$ clearly beating CHSH's critical detection of 83%, this is not a fair scenario since Bob is given a perfect detector. However we imposed linear inefficiency on Bob and showed a critical detection efficiency of 0.791% clearly outperforming CHSH. We emphasize that detection efficiency should be studied once given a specific experimental situation since these can vary significantly.

A remark on this: We have only been considering maximally entangled states in our studies. It is known that for CHSH-inequality, using partially entangled states one can lower the critical detection down to 67% due to Eberhard's inequality [40]. If anything similar is possible for our inequalities remains an open question.

The derivation of white noise tolerance of the inequalities showed that for a star-network of any number of sources we can keep the visibility per source constant and observe quantum correlations. Evidently the increased complexity of the system still allow the upper bound of noise-tolerance to be equivalent to that of the much less complex CHSH-inequality. This allows the practical construction of such star-networks. As for multipartite inequality we reproduce the strongest results of noise tolerance in Mermin inequality. Why star-networks yield nor stronger nor weaker critical bounds than ordinary Bell nonlocality is a central unsolved question in this thesis.

Despite presenting a violation for qutrit distribution in the bilocal scenario enforced through inequality (52) it is strongly believed that more powerful inequalities can be constructed. Studying the properties of star-networks with more than two-outcome measurements is still an open problem. It may be the case that a completely new approach to the problem is necessary.

For Bell nonlocality it is known to exist inequalities with a critical noise tolerance that improves with higher state dimensions [?]. Whether anything similar is possible in star-networks is an interesting question. Besides this motivation, strong qutrit inequalities may further reduce critical detection efficiency in two-outcome measurement scenarios. It is the authors conviction that such stronger Bell inequalities can be constructed.

A Lemma 1

Here we prove lemma 1.

Lemma 1: Let x_i^k be non-negative real numbers and $m, n \in \mathbb{N}$, then

$$\sum_{k=1}^{m} \left(\prod_{i=1}^{n} x_i^k \right)^{1/n} \leq \prod_{i=1}^{n} \left(x_i^1 + x_i^2 + ... + x_i^m \right)^{1/n} \tag{156}$$

Proof:

Make use of the elementary fact that the arithmetic mean is always larger than or equal to the geometric mean of a sequence. Exploit this fact to make m inequalities on the form

$$\prod_{i=1}^{n} \left(\frac{x_i^l}{x_i^1 + x_i^2 + ... + x_i^m} \right)^{1/n} \leq \frac{1}{n} \sum_{i=1}^{n} \frac{x_i^l}{x_i^1 + x_i^2 + ... + x_i^m} \tag{157}$$

for $l = 1, 2, ..., m$. Sum the left and right hand sides over the m inequalities

$$\begin{aligned} \sum_{l=1}^{m} \prod_{i=1}^{n} \left(\frac{x_i^l}{x_i^1 + x_i^2 + ... + x_i^m} \right)^{1/n} &\leq \frac{1}{n} \sum_{i=1}^{n} \sum_{l=1}^{m} \frac{x_i^l}{x_i^1 + x_i^2 + ... + x_i^m} \\ &= \frac{1}{n} \sum_{i=1}^{n} \frac{\sum_{k=1}^{m} x_i^l}{x_i^1 + x_i^2 + ... + x_i^m} = \frac{n}{n} = 1 \end{aligned} \tag{158}$$

Multiplication of both sides of eq.(158) with $\prod_{i=1}^{n} \left(x_i^1 + x_i^2 + ... + x_i^m \right)^{1/n}$ yields (156).

References

[1] A. Einstein, P. Podolsky, and N. Rosen, “Can quantum-mechanical description of physical reality be considered complete?” Phys. Rev., vol. 47, 777–780, (1935).

[2] E. Schrödinger, “Discussion of probability relations between separated systems,” Proc. Camb. Phil. Soc. 31, 555 (1935).

[3] J. S. Bell, “On the Einstein-Podolsky-Rosen paradox,” Physics, vol. 1, pp. 195–200, (1964)

[4] J. F. Clauser, M. A. Horne, A. Shimony, R. A. Holt, “Proposed experiment to test local hidden-variable theories,” Phys. Rev. Lett., vol 23, 880-884, (1969).

[5] A. Aspect, P. Grangier, and G. Roger, “Experimental realization of Einstein-Podolsky-Rosen-Bohm gedankenexperiment: A new violation of Bell’s inequalities,” Phys. Rev. Lett. 49, 91-94, (1982).

[6] A. Aspect, J. Dalibard and G. Roger, “Experimental test of Bell’s inequality using time-varying analyzers,” Phys. Rev. Lett 49, 1804 (1982).

[7] M. A. Rowe, D. Kielpinski, V. Meyer, C. A. Sackett, W. M. Itano, C. Monroe and D. J. Wineland, “Experimental violation of Bell’s inequality with efficient detection,” Nature, 409, 791-4, (2001).

[8] M. Giustina, A. Mech, et. al., “Bell violation with entangled photons, free of the fair-sampling assumption,” Nature, 497, 227-230 (2013).

[9] B. G. Christensen, K. T. McCusker, et. al., ”Detection-loophole-free test of quantum nonlocality, and applications,” Phys. Rev. Lett. 111, 130406 (2013).

[10] G. Wiehs, T. Jennewein, C. Simon, H. Weinfurter and A. Zeilinger, “Violation of Bell’s inequality under strict Einstein locality conditions,” Phys. Rev. Lett. 81, 23, 5039-5043, (1998).

[11] W. Tittel, J. Brendel, H. Zbinden, and N. Gisin, "Violation of Bell inequalities by photons more than 10 km apart", Phys. Rev. Lett., 81, 17, 3563-3566, (1998).

[12] T. Scheidl, R. Ursin, et al., "Violation of local realism with freedom of choice", Proceedings of the National Academy of Sciences, vol 107, 46, 19708-19713 (2010).

[13] S. Gröblacher, T. Paterek et. al., "An experimental test of non-local realism", Nature 446, 871-875 (2007).

[14] A. Aspect, "Introduction: John Bell and the second quantum revolution," Introduction Speakable and unspeakable in quantum mechanics. 2nd edition, Cambridge University Press.

[15] N. Gisin, G. Ribordy, W. Tittel and H. Zbinden, "Quantum cryptography," Rev. Mod. Phys. 74, 145 (2002).

[16] C. Bennett and G. Brassard, in Proceedings of the IEEE International Conference on Computers, Systems and Signal Processing, Bangalore, India (IEEE New York) pp. 175-179 (1984).

[17] A. Ekert, "Quantum cryptography based on Bell's theorem," Phys. Rev. Lett 67, 661-663 (1991).

[18] C. H. Bennet, G. Brassard and D. Mermin, "Quantum cryptography without Bell's theorem," Phys. Rev. Lett., 68, 557-559 (1992).

[19] D. Mayers and A. Yao, in Proceedings of the 39th IEEE Symposium on Foundations of Computer Science (IEEE Computer Society, Los Alamos, CA, USA, 1998), 503.

[20] M. A. Nielsen, I. L. Chuang, "Quantum computation and quantum information," Cambridge University Press (2000).

[21] J.-D. Bancal, N. Gisin, Y.-C. Liang, and S. Pironio, "Device-inedpendent witness of genuine multipartite entanglement, " Phys. Rev. Lett. 106, 250404, (2011)

[22] J. Barreiro, J. D. Bancal, et. al., "Device-independent demonstration of genuine multipartite entanglement," Nature Physics 9, 559-562 (2013).

[23] S. Perseguers, G. J. Lapeyre Jr, D. Cavalcanti, M. Lewenstein and A. Acín, "Distribution of entanglement in large-scale quantum networks," Rep. Prog. Phys. 76, 096001 (2013).

[24] C. H. Bennet, G. Brassard, et. al., "Teleporting an unknown quantum state via dual classical and Einstein-Podolsky-Rosen channels," Phys. Rev. Lett. 70, 1895-1899 (1993).

[25] C. J. Wood, R. W. Spekkens, "The lesson of causal discovery algorithms for quantum correlations: Causal explanations of Bell-inequality violations require fine-tuning," arXiv:1208.4119

[26] T. Fritz, "Beyond Bell's theorem: correlation scenarios," New J. Phys. 14 103001 (2012).

[27] T. Fritz, "Beyond Bell's theorem II: scenarios with arbitrary causal structure," arXiv:1404.4812

[28] J. Henson, R. Lal and M. Pusey, "Theory-independent limits on correlations from generalized Bayesian networks," arXiv:1405.2572

[29] C. Branciard, N. Gisin and S. Pironio, "Characterizing the Nonlocal Correlations Created via Entanglement Swapping," Phys. Rev. Lett. 104, 170401, 2010.

[30] C. Branciard, D. Rosset, N. Gisin and S. Pironio, "Bilocal versus nonbilocal correlations in entanglement swapping experiments," Phys. Rev. A., 85, 032119, 2012.

[31] J. Preskill, Course Notes for Physics 219: Quantum Entanglement, http://theory.caltech.edu/ preskill/ph229/.

[32] B.S. Cirel'son , "Quantum generalizations of Bell's inequality," Lett. Math. Phys. 4, 93-100, (1980).

[33] D. Greenberger, M. Horne and A. Zeilinger, "Bell's theorem, quantum theory, and conceptions of the universe," Dordrecht, 69-72 (1989).

[34] N. Brunner, D. Cavalcanti, S. Pironio, V. Scarani and S. Wehner, "Bell nonlocality," Rev. Mod. Phys. 86, 419 (2014).

[35] J. Calsamiglia, N. Lütkenhaus, “Maximum efficiency of a linear-optical Bell-state analyzer,” Appl. Phys. B 72, 67-71, (2001).

[36] N.D. Mermin, ”Extreme quantum entanglement in superposition of macroscopically distinct states,” Phys. Rev. Lett. 65, 1838 (1990).

[37] Z. Chen, ”Maximal violation of Mermin’s inequalities”, arXiv:quant-ph/0407029

[38] A. Garg and N.D. Mermin, ”Detector inefficiencies in the Einstein-Podolsky-Rosen experiment,” Phys. Rev. D 35, 3831-3835 (1987).

[39] P. H. Eberhard, ”Background level and counter efficiencies required for a loophole-free Einstein-Podolsky-Rosen experiment,” Phys. Rev. A 47, 747-750 (1993).

[40] D. Collins, N. Gisin, N. Linden, S. Massar and S. Popescu, ”Bell inequalities for arbitrary high-dimensional systems,” Phys. Rev. Lett. 88, 040404 (2002).